International Journal of Disaster Risk Reduction 28 (2018) 88–106

Contents lists available at ScienceDirect

International Journal of Disaster Risk Reduction

journal homepage: www.elsevier.com/locate/ijdrr

Life Cycle Cost and Return on Investment as complementary decision variables for urban flood risk management in developing countries

Raffaele De Risi[a,*], Francesco De Paola[b], Jane Turpie[c], Timm Kroeger[d]

[a] Department of Civil Engineering, University of Bristol, Queen's Building, University Walk, BS8 1TR Bristol, UK
[b] Department of Civil, Architectural and Environmental Engineering, University of Naples Federico II, Via Claudio 21, 80125 Naples, Italy
[c] Environmental Policy Research Unit, School of Economics, University of Cape Town, South Africa
[d] The Nature Conservancy, Global Science, 4245 North Fairfax Drive, Arlington, VA 22203, United States

ARTICLE INFO

Keywords:
Flood risk mitigation
Sustainable urban drainage systems
Green urban development
Cost-effectiveness
Natural infrastructure
Dar es Salaam

ABSTRACT

Herein we investigate Life Cycle Cost (LCC) and Return on Investment (ROI) as potential decision variables for evaluating the economic performance (ROI) and financial feasibility (LCC) of a set of flood mitigation strategies over time. The main novelty of this work is the application of LCC and ROI analyses at the urban level to an asset portfolio of flood-prone buildings. Reduced flood damage is treated probabilistically as avoided costs (LCC analysis) and returns (ROI analysis), respectively. The proposed methodology is applied to the case of Dar es Salaam, Tanzania, which suffers severe riverine flooding on a sub-annual basis. Specifically, LCC and ROI of five mitigation scenarios that include large-scale catchment rehabilitation, settlement set-backs and waste management are compared with the current situation. The main result is that the highest-performing flood mitigation option includes both conventional interventions and ecosystem rehabilitation.

1. Introduction

Riverine flooding is a worldwide threat to low-lying formal and informal built environments near watercourses that annually causes enormous human suffering, death and loss of livelihoods, damage to infrastructure and interruptions to economic activity [1]. Developing countries are particularly vulnerable to flooding impacts [2–5] for many reasons, including fragile economies [2], lack of risk awareness [6], preparedness and coping capacities [7], and lack of planning, implementation and enforcement of urban development, zoning regulations and building standards [8,9]. In many cities, this has led to largely unplanned and unmanaged urban growth characterized by poor or de facto non-existing construction standards [10,11], with informal settlements usually located in high-risk areas such as river banks and flood plains [12–14]. The result is large populations exposed to high hazard but characterized by low levels of resilience to natural disasters, a problem that is exacerbated by the increasing evidence of a correlation between climate change and extreme weather events [15,16].

Given this situation, it is of paramount importance to move forward from the classical flood protection paradigm to the new concept of flood risk management [17]. Quantification and communication of flood risk across an urban area and identification of potential mitigation strategies are activities that are fundamental for disaster risk management and for informing decisions by policy-makers and other stakeholders (e.g., local and national governments; bi- and multilateral funding agencies; civil society organizations, public planning, civil engineering and protection agencies) [18–20]; they are also an effective tool for reducing the gap between perceived and actual flood risk, in the short and long term [21,22], and for flood-risk communication across present and future stakeholders [23]. In this framework, the combination of risk assessment and Life Cycle Cost (LCC) analysis —or "integrated LCC analysis"— is an ideal instrument for quantifying the cost-effectiveness of Disaster Risk Reduction (DRR) measures, but also a powerful tool to communicate the results to stakeholders. LCC is a single benchmark performance metric indicating the total expected lifetime cost of a product, system, or structure [24]. The combination of risk assessment and life cycle considerations is not new as an environmental management system [25,26]; in fact, it has been used to quantify the environmental impact of mitigation strategies against natural hazards for single buildings [27,28], and is strongly recommended for flood control projects to ensure sustainability of the design outcomes [23]. Many studies have implemented LCC analysis and provide methodological approaches for its calculation in different civil engineering contexts and for different natural hazards [29–34].

The novel aspects of the work presented here are (1) the application of such an integrated LCC analysis to an entire flood-prone African

* Corresponding author.
E-mail addresses: raffaele.derisi@bristol.ac.uk (R. De Risi), depaola@unina.it (F. De Paola), jane.turpie@uct.ac.za (J. Turpie), tkroeger@tnc.org (T. Kroeger).

https://doi.org/10.1016/j.ijdrr.2018.02.026
Received 23 October 2017; Received in revised form 15 February 2018; Accepted 15 February 2018
Available online 21 February 2018

urban area to select the best flood risk mitigation strategy from a set of potential alternatives, and (2) the inclusion of conventional engineering-based, nature-based, and composite interventions. Such an assessment is the first step towards more sustainable urban development [35] and improved community resilience [36]. While sustainability and resilience encompass economic, environmental [37] and social aspects [38], here the focus is only an economic-financial one, which often is the binding constraint on projects especially in a lower-income country context. LCC analysis is a particularly appropriate tool for evaluating public investments in lower-income countries because it makes visible the full cost of a program over its lifetime. This ensures that decision-makers are aware of total financial commitments and can help avoid selection of less cost-effective alternatives characterized by lower initial but higher total costs that might result from a focus on initial costs only.

We also show that for natural hazard mitigation strategies whose benefits consist almost exclusively of avoided costs, LCC and Return on Investment (ROI) analysis yield identical preference rankings of intervention scenarios aimed at reducing flood damages. ROI analysis [39] is routinely applied in both the private and public sectors to evaluate the performance of competing investment opportunities and projects. However, it is equally suited to assessing the financial attractiveness of investments in natural infrastructure [40] and has been applied to catchment and coastal restoration [41–43].

We demonstrate the application of probabilistic LCC and ROI analyses by assessing the impact of different combinations of ecosystem rehabilitation, green engineering measures (collectively referred to as Green Urban Development (GUD) measures [44]) and conventional engineering interventions on probabilistically-estimated expected annual losses (*EAL*) from flood damage to the built environment in a section of Dar es Salaam, Tanzania, that is flooded on a sub-annual basis. To evaluate *EAL*, we adopt the performance-based methodology presented in De Risi et al. [3] and expand it to consider more than one structural building type (formal and informal masonry, reinforced concrete) and two limit states (LS), representing pre-defined damage states of the structures and their contents. Two main uncertainty sources are considered in this study: those related to the flood hazard and those associated with the structural vulnerability.

The methodology proposed herein is a unique multidisciplinary application and combination of methods that currently are generally disjointed. Given the modularity of the approach, as new models or improved data become available for individual steps in the methodology or for different geographical contexts, our model can be further improved or adapted to other sites. This compositional and spatial adaptability of the analytical procedure is another novelty of the work presented here, and the general principle of de-construction of risk problems fits perfectly within the disaster risk reduction practice and the performance-based engineering framework. Moreover, the methodology presented in this research was developed specifically to be applicable in a data-constrained developing country context. In particular, we identify several key open-source, freeware and government data resources needed for our and similar analyses. We note that an analysis like the one presented here should be complemented by an environmental and social impact assessment (ESIA; [45]) to provide a complete picture of all relevant impacts. While such an analysis is beyond the scope of this paper, in Section 4.5 we provide a brief discussion of the main expected environmental and social impacts of the scenarios evaluated here and argue why we expect them to be net welfare-enhancing overall. Nevertheless, an ESIA would allow identifying any risks of undesired distributional equity impacts that could be mitigated by appropriate policy interventions.

The focus of the analysis is the Msimbazi River which represents a constant flood threat to a large part of the center of Dar es Salaam, Tanzania, as exemplified by the six disastrous flood events experienced between 1995 and 2015 (1995, 1998, 2001, 2011, 2014, 2015) according to the EM-DAT disaster database [46]. Mitigating this flood risk is a key concern for the Kinondoni and Ilala district governments and the overarching Dar es Salaam metropolitan government [12]. The development of flood mitigation strategies for Dar es Salaam is also a priority issue for international organizations such as the World Bank and the U.K. Department for International Development [47]. We assess six scenarios: (a) the baseline scenario, which is the current situation; (b) creation of a setback zone around the river within the flood-prone area, including relocation of buildings from this zone, (c) application of GUD interventions in the Msimbazi catchment, (d) the combination of the previous two scenarios, (e) scenario *c* combined with off-line floodplain flood storage, and (f) a combination of scenarios *b* and *e*.

The paper is organized as follows. Sections 2 and 3 present the methodology and the case study, respectively. Section 4 describes the mitigation scenarios in detail and presents the results. Section 5 discusses the findings and presents conclusions.

2. Methodology

The two main inputs to LCC and ROI analyses for urban flood risk reduction strategies are comprehensive flood risk (i.e., hazard, vulnerability and exposure) assessments for each strategy and strategy implementation costs. Below we first present the methodology used for urban flood risk assessment, followed by the integration of the risk results into the decision variables.

2.1. Flood risk assessment in developing countries

2.1.1. Overview

Flood risk assessment encompasses hazard, exposure and vulnerability assessment [8,48]. Flood hazard is generally assessed through physically-based hydraulic models that estimate flood depth and velocity for each point within the study area and account for the presence of buildings and infrastructure and for soil characteristics (e.g. topography, permeability, etc.) [49]. The procedure adopted in this work for the hazard assessment is the same as in De Risi et al. [3] and is schematically represented in Fig. 1. The first step is the statistical description of precipitation trough rainfall curves, or Intensity-Duration-Frequency (IDF) curves (Fig. 1a), correlating rain duration, generally expressed in hours, with maximum rainfall intensity, typically expressed in millimeters per hour (mm/h). By analyzing past rainfall events, statistics of the recurrence of rainfall can be determined for various return periods T_R (e.g. 5, 10, 30, 50, 100, and 300 years), where T_R is the average time that passes between the occurrence of two rain events of a given intensity. Rainfall, geomorphological and biophysical data (topography, geo-lithology and land use, Fig. 1b) are used to characterize the hydrograph (Fig. 1c) and calculate the input discharge for different return periods. That volume is then propagated through the urban area by means of a hydraulic model (Fig. 1d) to obtain inundation maps corresponding to different return periods (Fig. 1e). These methods are generally computationally demanding and require significant amounts of data and parameters to describe the morphology, surface characteristics and drainage infrastructure of the modeling domain. However, the required data and modeling capabilities are not always available in lower-income countries [50]. Therefore, reasonable simplifications in modeling hypotheses and assumptions are generally accepted, especially in comparative scenario analyses that assess impacts in relative rather than absolute terms and adopt the same basic hypotheses across scenarios. For each single location, it is then possible to obtain a flood hazard curve (Fig. 1f), that is, the inundation depth versus its expected mean annual rate of occurrence, calculated as the inverse of the return period.

The exposure assessment (Fig. 1g) requires the identification of the human, built and natural elements at risk in the flooded area. Our analysis focuses only on the built environment due to the lack of information needed to comprehensively assess human health and indirect impacts. Nevertheless, to provide some perspective on the relative size

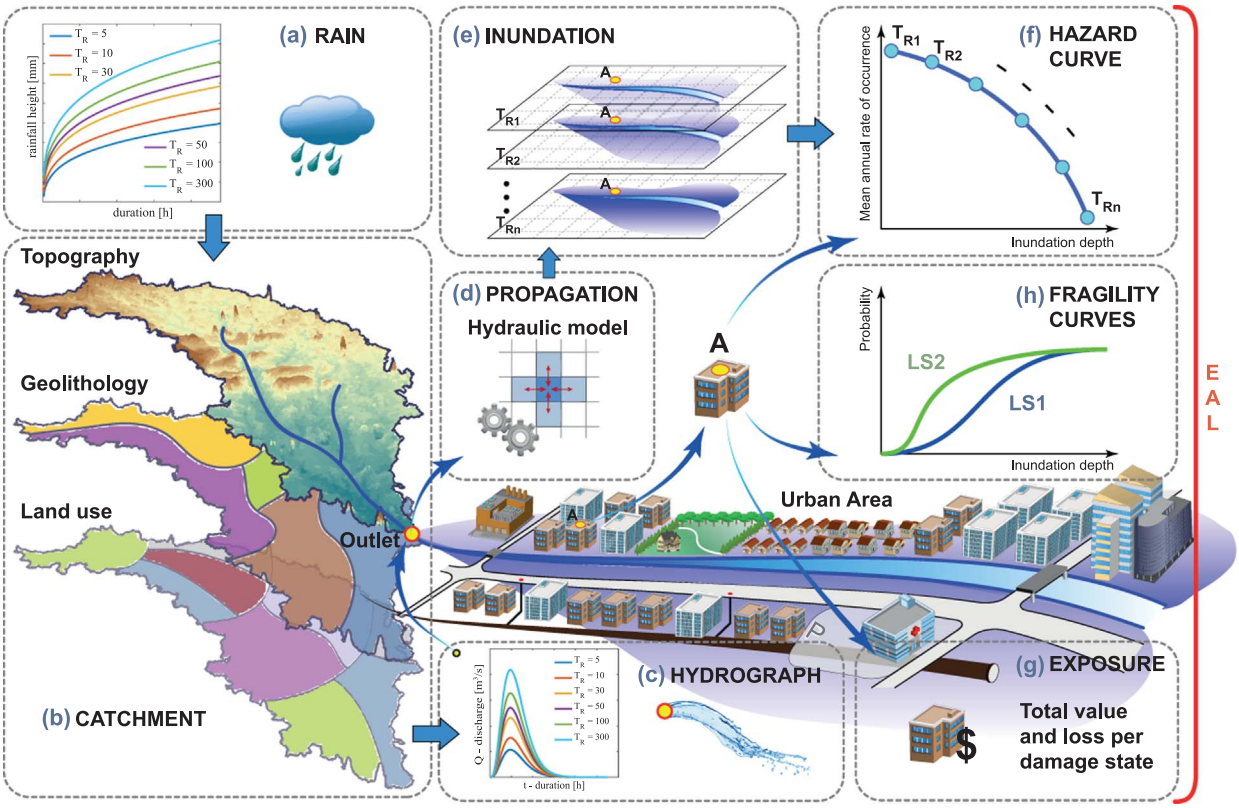

Fig. 1. The flood risk procedure.

of omitted flood impacts, we present findings from other studies (e.g., [51,52]) and construct lower-bound estimates of the cost of flood-related mortality and morbidity in Dar es Salaam.

Characterization of the built environment allows the application of a vulnerability analysis to quantify the adverse effects of flooding. The vulnerability analysis provides fragility functions (Fig. 1h), representing the probability of reaching or exceeding predefined damage states, for a given level of flood intensity (i.e., depth or inundation velocity) [53]. Applying the integration procedure proposed by De Risi et al. [3], the combination of hazard and vulnerability yields the mean annual rate of exceedance of a specific limit state, where limit state refers to a threshold for a structure beyond which it no longer fulfills a specified functionality. This rate can be further used to calculate the probability of exceedance in a given time window, by adopting a reasonable probability distribution describing the event occurrence. This probability can then be combined with the exposed asset value to quantify the flood damage risk in the predefined time window in terms of economic losses or in terms of number of casualties. The result is commonly expressed for a time interval of one year, as the Expected Annual Loss (*EAL*).

In this study two limit states are considered: the Collapse Limit State (CLS) and the Damage Limit State (DLS). The CLS represents a structural condition for which the bearing capacity of the building is no longer guaranteed (i.e. the structure is expected to collapse under the external actions). The DLS represents a situation in which the safety of occupants is guaranteed, but limited damage to structural and non-structural parts is expected (e.g. small or reparable cracks in the bearing structure and damage of building contents).

2.1.2. The risk integral

De Risi et al. [3] characterize flood risk assessment using a single equation:

$$\lambda_{LS} = \int P(LS|h)\cdot|d\lambda(h)| \tag{1}$$

where λ_{LS} denotes the risk expressed as the mean annual rate of exceedance of a given limit state (*LS*). $\lambda(h)$ denotes the mean annual rate of exceedance of a given flooding height h at a given point in the considered area. $P(LS|h)$ denotes the flooding fragility for limit state *LS* expressed in terms of the probability of exceeding the limit state threshold.

The risk λ_{LS} is calculated in terms of the mean annual frequency of exceeding the limit state *LS* for each node of the lattice covering the zone of interest by integrating fragility $P(LS|h)$ and the (absolute value of) hazard increment $|d\lambda(h)|$ over all possible flood height values. The mean annual frequency of exceeding the limit state λ_{LS} is then transformed into the annual probability of exceeding the limit state assuming a homogenous Poisson process as a model for occurrence of limit-state-inducing events:

$$P(LS) = 1 - \exp(-\lambda_{LS}\cdot t) \tag{2}$$

where t is the time in years. It should be noted that Eq. (1) divides the flood risk assessment procedure into two main modules: the hazard assessment module, which leads to the calculation of the mean annual frequency $\lambda(h)$ of exceeding a given flood depth h; and the vulnerability assessment module, used to calculate the flooding fragility curve in terms of the probability of exceeding a specified limit state $P(LS|h)$.

2.1.3. Expected annual losses

The costs of flooding can be broadly categorized into market versus non-market and direct versus indirect losses [54]. Direct market losses are negative impacts of the disaster itself on goods and services commonly bought and sold and whose value therefore generally can be fairly accurately determined using directly observable data (e.g., costs of infrastructure repair or medical treatment; reduction in firm output due to business interruption). Direct non-market losses are costs that are caused by the disaster itself but whose economic value cannot be readily quantified because they are not themselves traded on markets (e.g., suffering caused by injury or by death of family members or

friends; loss of life). While economic valuation of direct non-market impacts is possible (e.g. suffering from specific health effects) and in many cases even fairly common (e.g., the value of a statistical life or of disability-adjusted life years), the resulting values often are contentious because they rely on indirect valuation approaches that utilize individuals' stated rather than observed preferences, or because many individuals are uncomfortable with assigning monetary values to these impacts. Indirect losses are not caused by the immediate disaster itself but rather by secondary effects. For example, if flooding damages infrastructure (e.g. transportation or utility networks), it often causes business interruptions that continue far beyond the duration of the actual flooding itself. Likewise, because of economic linkages among businesses and economic sectors, flooding may cause indirect losses in the form of negative effects on economic activity outside of the flooded area. Our analysis only considers direct market losses from flooding in the form of damage to buildings, which is relatively well-studied as it is the most important parameter for the insurance industry [55]. In Section 4.3 we discuss literature findings on how direct structural damages to buildings compare to total flood damages.

The expected loss is calculated as the expected repair cost (per building or per unit residential area), $E[R]$, as a function of the limit state probabilities (change in probability of exceedance) and by defining the i^{th} damage state as the structural state between limit states i and $i + 1$:

$$E[R] = \sum_{i=1}^{N_{LS}} [P(LS_i) - P(LS_{i+1})] \cdot R_i \tag{3}$$

where N_{LS} is the number of limit states that are used in the problem in order to discretize the structural damage, R_i is the repair cost corresponding to the i^{th} damage state, and $P(LS_{N_{LS}+1}) = 0$. In this study, repair costs associated with the *CLS* are set equal to 100% of the value of the total exposed asset, and the repair costs associated with the *DLS* to 50% of that value. The distinction among the asset values associated with the onset of the different limit states (i.e. 50% of the total asset in the case of *DLS*; 100% in the case of *CLS*) is a well-established practice in the risk assessment literature for many natural hazards, such as floods [56,57], earthquakes [58] and tsunamis [59]. Finally, in the case of collapse, a further cost of 10% of the entire asset [28,30] is considered for the dismantling of the collapsed building and removal and disposal of debris [60]. The *EAL* then is obtained using probability terms in Eq. (3) calculated considering a time window of one year in Eq. (2).

2.2. Life Cycle Cost

The LCC concept was developed as a financial technique for ranking investments, and in the last thirty years has been gaining prominence in the building and environment fields, too, since it has been linked to resilience and sustainability [23]. In fact, civil structure and infrastructure sustainability and resilience have been identified as grand challenges for engineering in the 21st century [61].

ISO 15686 Part 5 [62] Life Cycle Cost Analysis specifies that for buildings and other constructed assets, the LCC takes into account all significant and relevant costs over the asset's life that are incurred to achieve defined levels of performance, including reliability, safety and availability over the period of analysis. Therefore, for a given structure, LCC consist of the sum of the present value (*PV*) of all expected costs from construction to the end of the life span of a structure, including construction cost, inspection and maintenance cost, repair or replacement cost and disposal costs.

Costs can be divided into four major categories, based on whether they are planned or unplanned, and whether they are sustained by the owner of the structure/infrastructure or its user. The latter distinction often is complicated in the case of public infrastructure [63]. The scenarios evaluated in our analysis comprise both public (GUD interventions; setbacks) and private (housing structures) LCC components. Planned costs arise from construction, maintenance, and retrofit; unplanned costs are related to damage from exceptional events such as natural hazards. Because of the many uncertainties in assessing the LCC of buildings (e.g., the durability and aging of construction materials, buildings, and their effect on maintenance costs; the occurrence and severity of natural events impacting the structure and associated unplanned costs; a change in the life-time of the asset due to, for example, a change in functionality), LCC is evaluated in a probabilistic framework as the expected value (E[·]) of costs (C) in a time interval (T) equal to the life cycle (LC) of the structure:

$$E[C|T = LC] = C_0 + C_I + C_M + C_R + C_D \tag{4}$$

where C_0 is the initial construction cost, C_I is the inspection cost, C_M is the maintenance cost, C_R is the repair/replacement cost, and C_D is the down-time cost (i.e. the cost associated with the suspension of the economic activities related to the asset; omitted here).

Construction cost (C_0) represents the initial investment. In the past, and in many cases today, construction cost often was the only cost considered in decision-making processes [63,64].

Inspection costs (C_I) and maintenance costs (C_M) are planned costs incurred by users or owners. Those costs are expected to occur at regular time intervals and are necessary to keep the structure/infrastructure functional during its lifetime; however, the length of these intervals and the amount of recurrent inspection or maintenance varies among different types of structures. One possible approach to estimating C_I and C_M is to plan maintenance actions in advance using empirically-based methodologies that draw on large databases to determine the optimal maintenance plan given the specific characteristics of a particular type of structure [65]. Once the expected number of inspection and/or maintenance events is calculated, it is possible to estimate mean annual inspection (C_i) and maintenance (C_m) cost. We adopt the common practice of assuming C_i and C_m as a percentage of the initial intervention cost [65]. Discounting and integration of mean annual inspection and maintenance costs over T yields their estimated present values C_I and C_M:

$$C_I = \sum_{t=1}^{T} \frac{C_i}{(1 + \xi)^t} \tag{5}$$

$$C_M = \sum_{t=1}^{T} \frac{C_m}{(1 + \xi)^t} \tag{6}$$

In Eqs. 5 and 6, the denominator is the cost discount factor used to calculate PV cost, and ξ is the annual discount rate. A recent study [66] estimates Tanzania's social consumption discount rate (the rate that should be used for evaluating long-lived public investments) to be 4.9%, close to the 5% typically adopted for civil structures [67]. In this study, we conservatively assume that $\xi = 6\%$. Because the choice of discount rate can significantly affect both C_I and C_M [33] we include this parameter in our sensitivity analysis considering two additional discount values, 5%, and 7%, respectively.

Risk from natural hazards is integrated into LCC through C_R which are unplanned and correspond to the PV *EAL*:

$$C_R = \sum_{t=1}^{T} \frac{EAL}{(1 + \xi)^t} \tag{7}$$

where *EAL* is the stream of equal expected annual expenditures necessary to repair/replace the structure in question and t is the time in years up to the reference life T of the structure and is estimated as described in De Risi et al. [3].

2.3. Return on Investment

We calculate ROI as the benefit-cost ratio of an investment:

$$ROI = \frac{Benefit}{Cost} \tag{8}$$

where the benefit of implementing a flood mitigation strategy S_i is the difference between the PV *EAL* of the baseline (S_0) and intervention (S_i) scenarios, respectively:

$$Benefit_{Si} = PV(EAL_{S0}, t) - PV(EAL_{Si}, t) = \sum_{t=1}^{T} \frac{EAL_{S0}}{(1+\xi)^t} - \sum_{t=1}^{T} \frac{EAL_{Si}}{(1+\xi)^t} \tag{9}$$

As in LCC analysis, the costs of S_i include not only initial implementation cost C_0 but also ongoing inspection (C_I) and maintenance (C_M) costs:

$$Cost_{Si} = C_{0,S_i} + C_{I,S_i} + C_{M,S_i} = C_{0,S_i} + PV(C_i, t) + PV(C_m, t) = \\ = C_{0,S_i} + \sum_{t=1}^{T} \frac{C_i}{(1+\xi)^t} + \sum_{t=1}^{T} \frac{C_m}{(1+\xi)^t} \tag{10}$$

Substituting Eqs. (9) and (10) into (8), ROI can be expressed as

$$ROI = \frac{PV(EAL_{S0}, t) - PV(EAL_{Si}, t)}{C_{0,S_i} + PV(C_i, t) + PV(C_m, t)} \tag{11}$$

The payback period ($T_{ROI\ =\ 1}$) is the time necessary for intervention ROI to reach unity. This is the point at which the PV of the cumulative benefits surpasses the PV of the cumulative costs of the intervention. The ROI is less than unity if the PV of implementation costs of the intervention exceeds the reduction the intervention produces in the PV of expected annual losses. Because ROI does not indicate the absolute size of net benefits, a complete analysis must also calculate the Net Present Value (NPV) of the scenarios (i.e. the difference between discounted streams of annual costs and benefits).

2.4. Comparison of LCC and ROI

Fig. 2 presents a schematic representation of the relationship between LCC and ROI for two hypothetical mitigation strategies *S1* and *S2*. The points at which LCC_{S1} and LCC_{S2} intersect the LCC of the baseline scenario (*S0*) represent the payback periods of the intervention scenarios. To the right of $T_{ROI}(S1)$ and $T_{ROI}(S2)$ the ROI exceeds unity and the intervention scenarios produce net benefits.

This can readily be demonstrated analytically using Eq. (11). ROI exceeds 1 if the numerator exceeds the denominator, that is, if the PV of the avoided losses due to the mitigation exceeds the PV of mitigation costs:

$$PV(EAL_{S0}, t) - PV(EAL_{Si}, t) > C_{0,S_i} + PV(C_i, t) + PV(C_m, t) \tag{12}$$

Likewise, the LCC of the baseline scenario (LCC_{S0}) exceeds that of the mitigation scenario (LCC_{Si}) if

$$PV(EAL_{S0}, t) > PV(EAL_{Si}, t) + C_{0,S_i} + PV(C_i, t) + PV(C_m, t) \tag{13}$$

Eqs. 13 and 12 are identical, demonstrating the consistency of LCC and ROI for ranking mitigation strategies.

Fig. 2 shows that even though hypothetical mitigation strategy *S1* has a lower initial cost, strategy *S2* is preferable on financial and economic grounds since it requires a shorter payback time, has a lower LCC and a greater ROI for any time period exceeding its payback period.

It is worth emphasizing that LCC and ROI analyses yield identical rankings of alternatives only if the public policy or program being evaluated produces benefits only in the form of avoided costs. The presence of other types of benefits breaks the equivalence of LCC and ROI. For example, if some of the policy alternatives produce productivity gains, the latter would be reflected in their ROI, but not in their LCC. Because public policies such as flood mitigation must be evaluated on the basis of their full social impacts, if those impacts include benefits other than avoided costs, LCC generally will only be able to identify the financially preferred (least-cost) but not the optimal (i.e., social welfare-maximizing) alternative. In cases where some policy alternatives produce sizeable benefits beyond avoided cost, LCC therefore must be complemented by a social ROI analysis, that is, a social benefit-cost analysis. Furthermore, because ROI is the benefit-cost ratio and thus does not indicate the size of the net benefits a policy alternative produces, any evaluation of flood mitigation policies should also include their net present value (NPV), that is, the difference between the sums of discounted streams of benefits and costs over time.

3. Case study

Dar es Salaam, the largest city in Tanzania, has experienced rapid population growth with a current estimated population of 4.4 million. Most of this growth has taken the form of unplanned and informal residential areas, with 75% of the area under informal development, and many houses being built in areas previously considered unsuitable, such as below flood lines on floodplains and abutting river edges. City infrastructure has not been able to keep up with population growth, with the majority of residents lacking access to public services including sanitation and waste collection [47]. During the rainy season, intense rainfall events often cause severe flooding in parts of the city. Flooding problems are greatest along the Msimbazi river, which floods part of the city center and is the focus of this case study.

3.1. Flood hazard

3.1.1. Available data

In this study, historical rainfall data (Fig. 3a) were obtained from the single existing meteorological station in the catchment, located at Dar es Salaam international airport at 55 m above sea level, 6°86'S and 39°20'E. A detailed description of the data and the statistical treatment applied to derive the intensity duration curves (Fig. 3b) can be found in De Paola et al. [68].

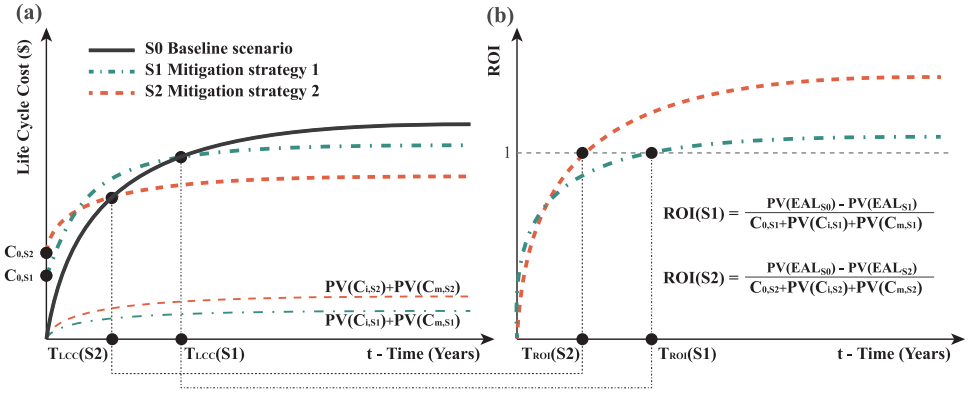

Fig. 2. Schematic representation of LCC and ROI for two alternative mitigation strategies S1 and S2.

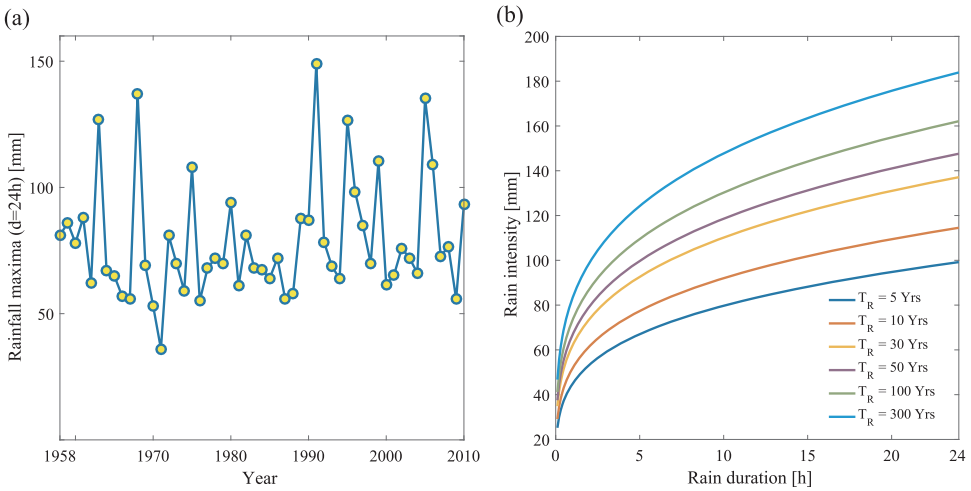

Fig. 3. (a) Historical rainfall data and (b) IDF curves.

The geomorphological data used in this analysis are topographic (digital elevation model (DEM), Fig. 4a), land use (Fig. 4b), geologic (Fig. 4c) and geo-lithologic (Fig. 4d). The adopted DEM has a 2-m horizontal resolution and is obtained by combining in a mosaic three datasets: (i) a 30-m resolution DEM obtained from the U.S. National Aeronautics and Space Agency (NASA) Shuttle Radar Topography Mission (SRTM) project website (http://gdex.cr.usgs.gov/gdex/); (ii) a contour map with 2-m vertical resolution covering only the central part of the city, acquired from the Dar es Salaam city council; and (iii) ten 50-cm resolution LIDAR surveys for strategic areas in the city of Dar es Salaam, obtained from a previous research project. Details on the constructed DEM can be found in [47]. The final DEM is used to identify the catchments feeding the river system (upstream of the outlets) considered in the analyses, and as basic information for the inundation simulations (downstream of the outlets). Three catchments are identified, C1, C2 and C3 (Fig. 4a), feeding the main Msimbazi, the Kibangu, and the Ng'ombe water courses, respectively.

We use two resources to characterize land use: (i) a coarse-resolution map made available by the International Livestock Research Institute (http://192.156.137.110/gis/search.asp?id=543) showing the land use for the entire country in 2002; and (ii) a finer-resolution map of the city of Dar es Salaam obtained from the Climate Change and Urban Vulnerability (CLUVA) project (www.cluva.eu). The latter is a map of Urban Morphology Type (UMT), which is a powerful tool for the representation of the built and natural environment because it brings together facets of urban form and functions [69]. The use of these two land use data sets was necessary because the main catchments feeding the Msimbazi river extend beyond the limit of the more refined UMT map, which is confined to the political boundaries of Dar es Salaam.

The source data for the geologic and geo-lithologic maps were acquired from the Geological Survey of Tanzania's Geological and Mineral Information System (http://www.gmis-tanzania.com/). These maps have a resolution of 1:2 M, are the official maps recognized by the Republic of Tanzania and represent the best data available for the country; moreover, they are in good accordance with the ISRIC – World Soil Information data (http://www.soilgrids.org/).

3.1.2. The hydrographs

Several rainfall-runoff methods can be used to construct hydrographs: the Rational Method [70], the Curve number Method [71], or more sophisticated approaches such as distributed/semi-distributed models [72]. The more sophisticated the method, the more data is required to calibrate model parameters [73]. One of the main advantages of distributed models is that they allow predictions of hydrologic variables at interior points [73]. However, in our study we are only interested in streamflow near the flood-prone outlet. Importantly, comparing a complex distributed model, a lumped conceptual model, and an intermediate complexity model in data-sparse catchments in Zimbabwe, Refsgaard and Knudsen [74] found that without calibration, the distributed models performed only marginally better than the lumped model, concluding that their results could not strongly justify the use of the complex distributed model. There is one fully-distributed model, WaterWorld [75], that runs on remotely-sensed global data sets and thus does not require local gauge and meteorological data. However, WaterWorld only predicts mean water balance and only at a monthly time step, making it unsuitable for flood modeling.

In lower-income countries, model choice often is constrained by the lack of data necessitating use of relatively simple approaches. For ungauged basins (i.e. where discharge measurements are unavailable) such as those of Dar es Salaam, the classic Curve Number Method (CNM) is considered suitable for modeling the hydrograph. The main advantages of the CNM are that: (a) it is the simplest conceptual method for estimating the direct runoff amount from a rainfall event, and is well supported by empirical data; (b) it relies only on one number, the curve number CN, which is an integrated representation of the main watershed characteristics affecting runoff; (c) it is fairly well documented for its inputs, that is, data needed to calculate CN generally are readily available (soil, land use, surface conditions, and antecedent moisture conditions); and finally (d) its features are readily grasped, well established, and accepted not only in the U.S. (where the methodology originally was developed) but also other countries around the world.

The principal limitations of the CNM are that (a) rainfall is considered spatially and temporally uniform; (b) there is a lack of clear guidance on how to set antecedent soil moisture conditions (AMC) to reflect empirical conditions, especially for lower CN and rainfall amounts; and finally, (c) the method was originally developed for agricultural areas, and while it generally also performs well in other contexts, it performs less well for forests. Fig. 5a-c show the hydrograph obtained for the three catchments considering a soil with moderate infiltration rate (soil category B) and AMC III (wet condition), the second-most common condition in the Msimbazi watershed during the growing season according to Jalayer et al. [16] (Fig. 5d). In De Risi et al. [3] the detailed procedure employed to obtain such hydrographs is explained. We use AMC III rather than the most common condition, AMC I (dry), in order to generate conservative estimates of intervention impacts. Under wet soil conditions, the increment in soil infiltration capacity produced by the land cover change (bare, low vegetation, crops or pasture to forested) declines [76], because unlike under bare [77] or agricultural cover [78], under forest cover surface runoff only occurs with much higher rainfall and soil moisture content [79].

To simulate the effect of the interventions on the hydrograph, we first calculate the weighted mean CN of each catchment using the

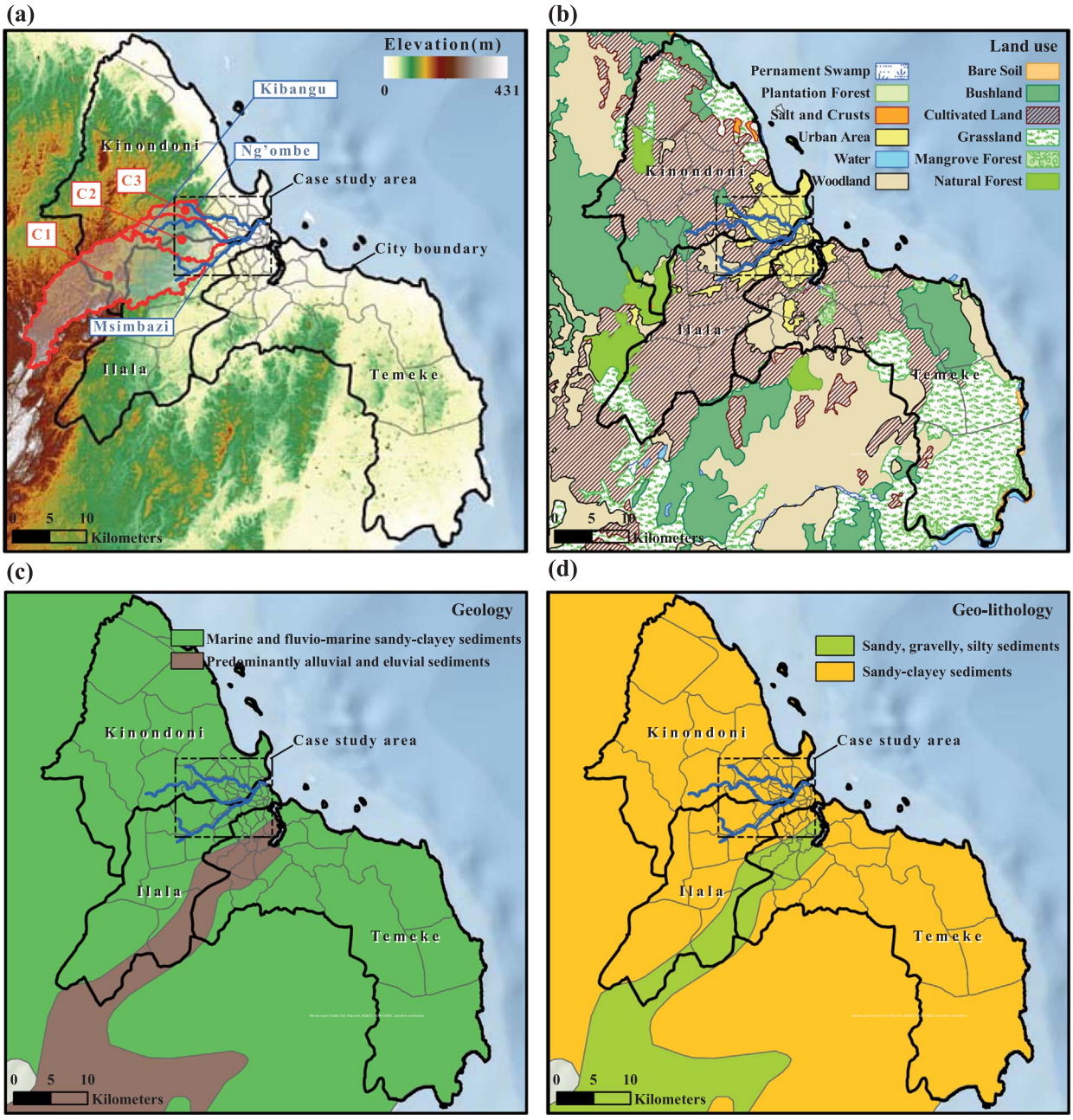

Fig. 4. The city of Dar-es-Salaam: (a) elevation, considered rivers and their catchments; (b) land use; (c) geology and (d) geo-lithology.

current percent shares and CNs of each land cover/use and soil category B, with standard CNs adjusted to AMC III. We then recalculate mean weighted CNs for each catchment for a situation where land cover/use has been modified by the GUD interventions described in Section 4. The resulting estimated change in weighted mean CNs is approximately equivalent to a change in infiltration rate from moderate to high [71]. Fig. 5e shows how beneficial effects induced by interventions (explained in the following) are modeled. Increase in soil permeability is modeled by changing the infiltration rate from moderate to high (i.e. changing soil category from B to A). The red curves in Fig. 5e show the modified hydrographs for catchment 1 due to soil permeability improvement. Similarly to [16], the hydrologic improvement is modeled by changing AMC from III to II instead of changing the soil type from B to A to reflect increased permeability. The effect on the final hydrographs is comparable to that of varying soil type (black curves in Fig. 5e).

It is very important to underline that in the absence of additional data (infiltration capacity; higher spatial resolution precipitation; stream flow), and using the CN method, the improvements can be modeled only in such a lumped way by modifying the input hydrograph.

3.1.3. Inundation maps

In this study, two-dimensional flood routing is accomplished through the numerical integration of the equations of motion and continuity (dynamic wave momentum equation) for flow. The numerical simulation is implemented using the commercial software FLO-2D [49], a flood volume conservation model based on general constitutive fluid equations of continuity and flood dynamics, that is, shallow water equations or Saint-Venant equations. The flow is considered variable in space and in time, and the bottom friction is evaluated using Manning's formula. The Manning's coefficients were assigned to computational cells based on a literature review. Conservative estimates of 0.04 and 0.02 were assumed for natural and urban areas, respectively [80].

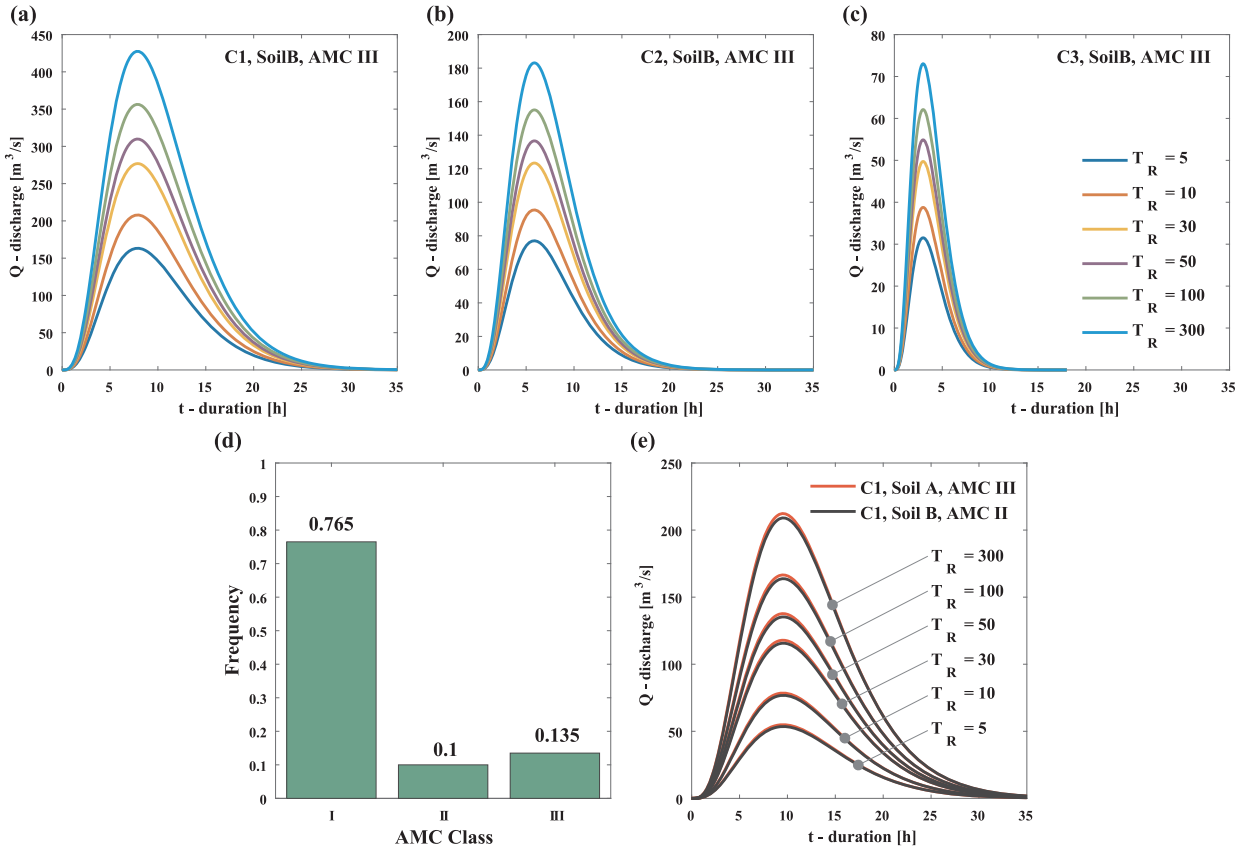

Fig. 5. Hydrographs for (a) catchment 1, (b) catchment 2, and (c) catchment 3; (d) histogram of the AMC classes for the growing season; (e) hydrographs for the improved catchment C1.

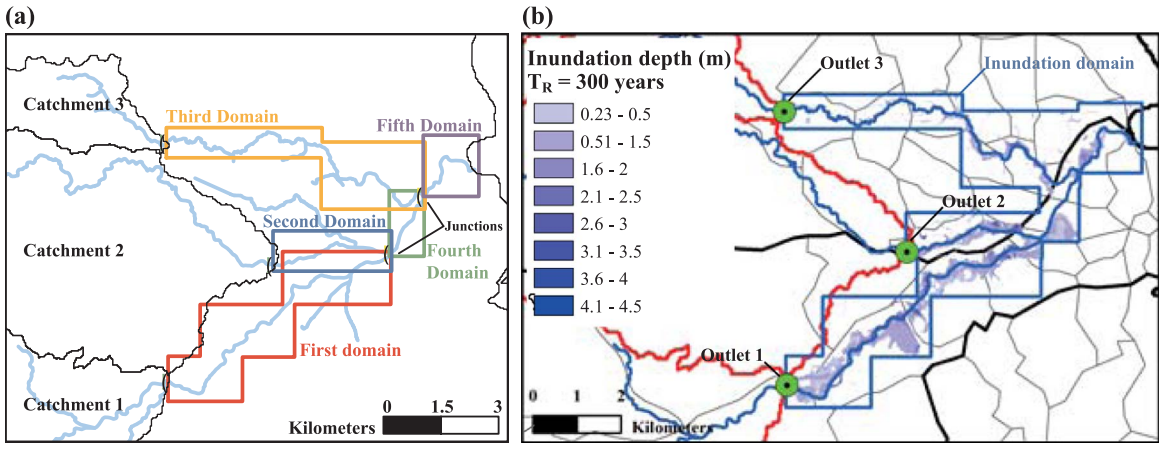

Fig. 6. (a) Analysis sub-domains, and (b) inundation map for T_R = 300 years.

Drainage infrastructure not captured in the DEM (e.g., the sewage system) was omitted due the lack of available data on these systems. The simulation duration for each sub-domain is equal to the time necessary to exhaust the related hydrograph. Given the large size of the case study area, the analysis domain was divided into five sub-domains in order to reduce computation time (Fig. 6a).

The first, second and third sub-domains correspond to the three main water courses; the last two sub-domains are defined areas downstream of the junctions of those main water courses. In each drainage outlet, the respective modeled hydrograph was applied; in each junction, a hydrograph was obtained as the sum of the flows from the upstream water courses. Fig. 6b shows the inundation scenario for a return period of 300 years. The inundation results in terms of flood depth and velocity for all sub-domains can be found in [47]. In all analyzed sub-domains, a large part of the built environment is affected by flood events. The next section presents the methods used to identify and classify the exposed assets.

3.2. Exposure

The inundation domain covers a large part of the city center in which residential structures and economic activities are concentrated (Fig. 7a). In this study, all buildings in the inundation domains are included in the exposure analysis.

Building-by-building spatial identification (black polygons in Fig. 7a) benefits from Volunteered Geographic Information (VGI); specifically, OpenStreetMap (OSM, www.openstreetmap.org), one form of crowdsource big data, which is very useful in lower-income countries

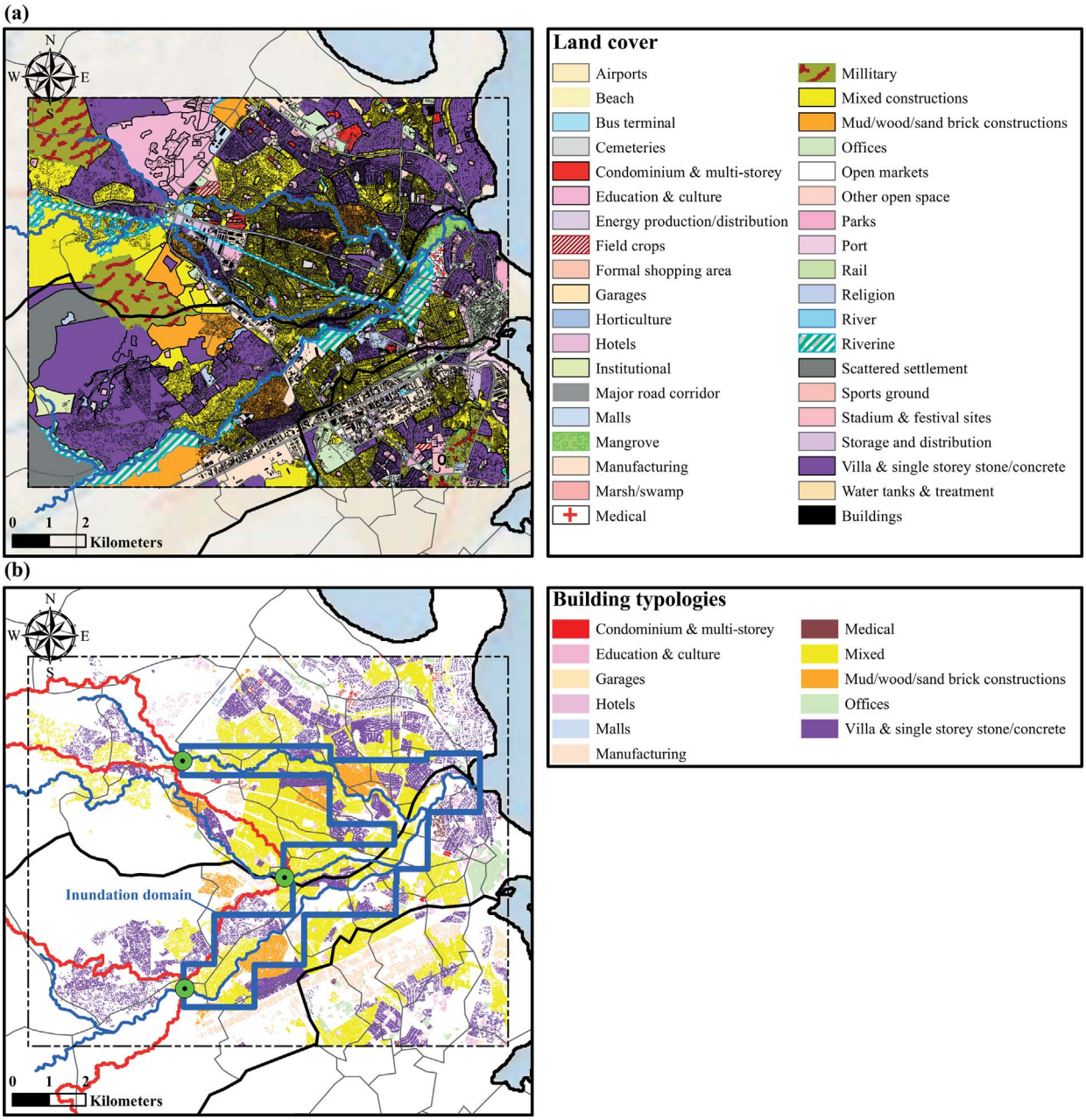

Fig. 7. (a) Land use in the case study area, and (b) building typology. (For interpretation of the references to color in this figure, the reader is referred to the web version of this article.)

often characterized by a lack of data on exposed assets. By intersecting the land cover map with building footprints, it is possible to identify the type of each building. Fig. 7b shows the buildings in the inundation domain (a total of 209124) and the distribution of footprints by building type.

The buildings at risk in the inundation domain are identified by intersecting the building map with the maximum extent of the baseline flood inundation corresponding to the maximum return period considered (300 years in this study). A total of 12,744 buildings fell within this area (Fig. 8a).

Information on building characteristics led to the identification of three main structural typologies (Fig. 8b-d): informal masonry (IM); formal masonry (FM); and reinforced concrete frames (RCF). Based on a recent survey of building values in Dar es Salaam (Appendix A), building values by structural typology and use type are calculated and presented in Table 1. More details on the procedure used can be found in [47].

Fig. 8d shows the distribution of building structural types, indicating that almost 90% of all buildings in the flood domain are classified as Informal masonry.

3.3. Vulnerability

The structural vulnerability is described using fragility functions. A fragility function evaluates the probability of reaching or exceeding specific damage states (ds) for a given hazard intensity [53]. Such relationships between hazard and potential damage play a vital role in quantifying damage and losses associated with flood events. In this

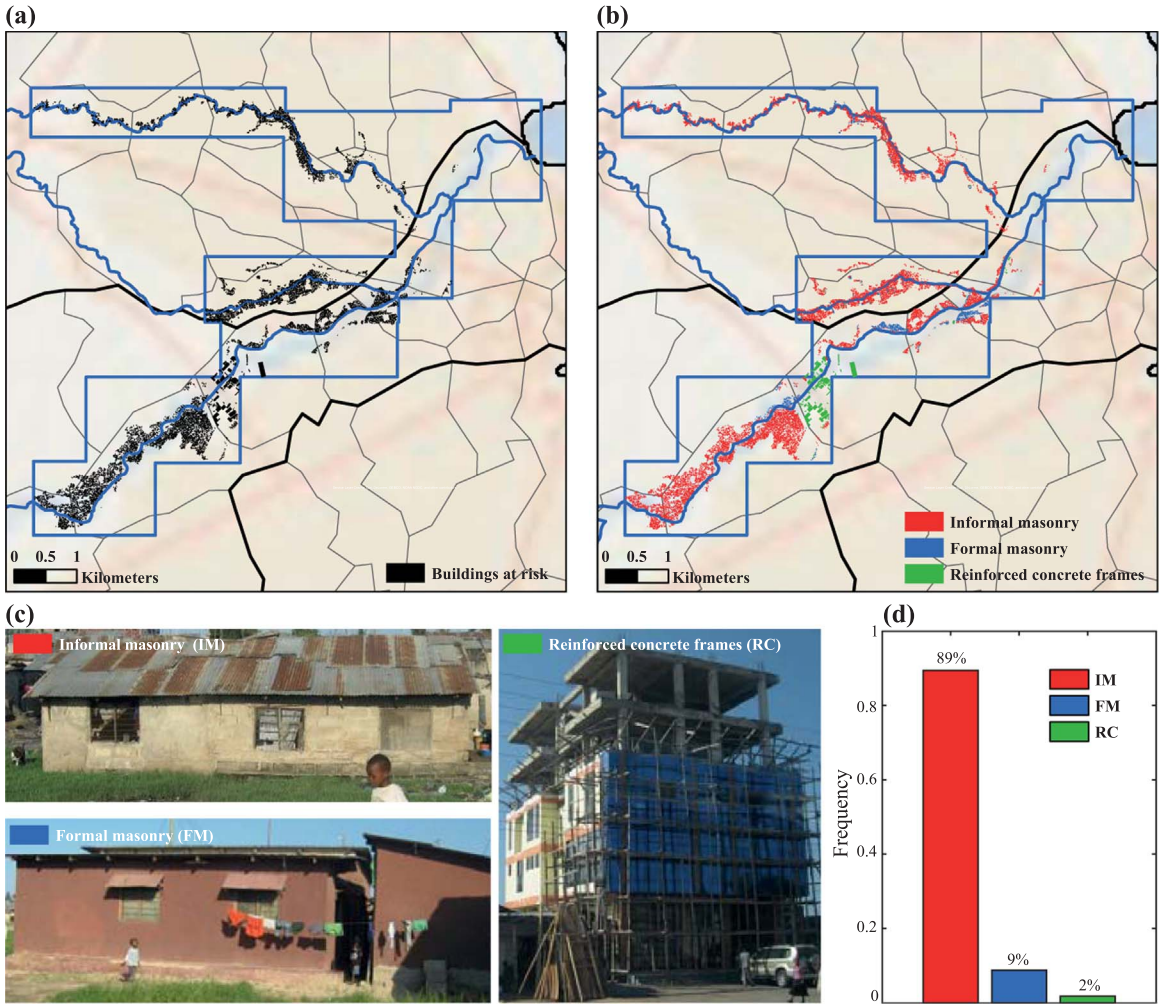

Fig. 8. (a) Buildings at risk, (b) structural typology of buildings at risk, (c) pictures and (d) distribution of the three main structural categories.

Table 1
Unit construction costs for different building typologies in Dar es Salaam.

Building type	US$/m^2
Informal Masonry residential	120
Formal Masonry residential	150
Informal Masonry commercial	472
Formal Masonry commercial	374
Reinforced Concrete Frame commercial or residential	745
Reinforced Concrete Industrial	858

study, specific fragility models considered suitable for Dar es Salaam are adopted; fragilities are modeled as log-normal functions completely defined by the median (η) and the logarithmic standard deviation (β). Eq. (14) shows the classical formulation where $\Phi(\cdot)$ denotes the standard Gaussian (Normal) cumulative probability distribution.

$$P(DS \geq ds|h) = \Phi\left(\frac{\ln h - \ln \eta}{\beta}\right) \quad (14)$$

We use Jalayer et al.'s [81] flooding collapse fragility functions for typical low-standard structures in Dar es Salaam for describing the vulnerability of IM buildings in the city. To obtain the damage fragility function, according to the results presented in De Risi [82], the median value corresponding to the collapse limit state is divided by two, and the logarithmic standard deviation is kept the same. For the FM structures, Reese et al. [83] developed empirical fragility functions for residential masonry buildings with respect to the hydraulic action induced by tsunamis. The use of tsunami fragility curves can be considered valid since the empirical fragility curves are obtained considering aggregated data for which the median flow velocity values are usually not very high, ranging from 2 m/s to 5 m/s [84], values that are comparable with the velocity values obtained with the current simulations in Dar es Salaam. In Reese et al. [83], fragility curves are obtained for five different damage states that include two that correspond to the two limit states considered here, DS3 (equivalent to DLS) and DS5 (equivalent to CLS). Finally, for RCF structures, Suppasri et al. [85] developed empirical fragility functions for RC buildings for the action induced by tsunamis. We average the statistics for their 1-storey and 2-storey buildings. Among the six damage states presented, only the curves associated with DS3 (i.e., DLS) and DS5 (i.e., CLS) are considered. Table 2 lists the statistical characteristics of the three sets of fragility curves, and Fig. 9 shows the fragility curves for the three

Table 2
Fragility curve parameters by structural type and limit state.

Type	Limit state	η [m]	β
IM	DLS	0.42	1.52
	CLS	0.84	1.52
FM	DLS	1.28	0.35
	CLS	2.49	0.50
RCF	DLS	1.20	0.79
	CLS	5.60	0.81

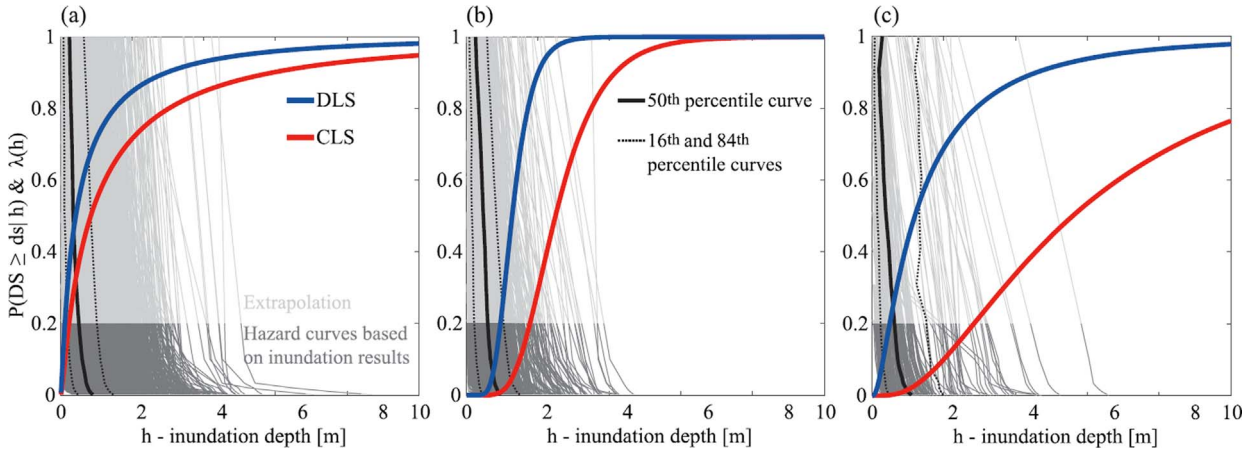

Fig. 9. Fragility curves and hazard curves for (a) IM buildings, (b) FM buildings, and (c) RCF buildings. The dark grey part of hazard curves is calculated; the light grey part is extrapolated.

structural typologies analyzed and the hazard curves obtained by interpolating inundation maps with building locations and types.

3.4. Expected annual loss

Integrating the fragility and hazard curves leads to an EAL of US$ 47.30 million in the baseline scenario S0.

4. Mitigation strategies: scenarios and results

This section presents potential mitigation strategies, discusses their implementation in the model and their effect on the hazard, and evaluates their LCC and ROI.

Urban drainage management has evolved significantly over the last few decades, from a conventional 'rapid disposal' approach to a more integrated and sustainable 'design with nature' approach. Examples of this new approach include Integrated Urban Water Management (IUWM), Water Sensitive Urban Design (WSUD), urban storm-water Best Management Practices (BMPs), Sustainable Urban Drainage Systems (SUDS) and Low Impact Development (LID). All of these comprise portfolios of measures to address flooding and/or water quality problems. These tend to be categorized into passive and active structural and non-structural measures. Active measures, which seek to reduce the effects of urbanization on the quantity and quality of catchment runoff, can be further categorized into source, local and regional controls [86]. With the feasibility of source controls (permeable pavement, infiltration trenches, green roofs, subsurface soakaways, rainwater harvesting) in our study area limited by lack of available space, soil and building characteristics as well as comparative cost-effectiveness, non-structural measures were identified as the most suitable flood management options. Specifically, we considered the protection, restoration and/or enhancement of natural systems, a river cleaning program and the improvement of solid waste management [47]; these measures are collectively referred to as Green Urban Development (GUD) measures here. There are substantial areas of degraded forest in the catchment that could be restored, and floodplains lower in the catchment have been artificially disconnected from the river, greatly reducing their potential for flood mitigation and co-benefits. Restoring the natural hydrological connectivity of the river system would provide numerous ecological benefits and the deepening of the floodplain in the lower catchment provides an opportunity to develop a wetland park which would provide inner city recreational green open space. Furthermore, there are several floodplain areas in the mid-lower catchment that could be enhanced to improve their water holding capacity while at the same time providing other benefits such as erosion control and provision of areas for agriculture and wetlands. The idea of a mixed use enhanced riparian and floodplain area was developed based on the concept of a combination of riparian zone rehabilitation and floodplain enhancement measures that store and retard flows but that could easily include opportunities for other beneficial uses, including sports fields, agricultural lots and parks as well as active riparian buffer zones or conservation corridors. Whilst these beneficial floodplain uses raise initial costs, it is expected that they are likely to reduce opportunities for unplanned resettlement of the floodplain. In addition, a community-based river cleaning program was included as an essential measure to help deal with the problem of solid waste in the river system that leads to the clogging of drainage infrastructure such as culverts and channels. This could be considered as an interim measure until improved municipal waste collection and management services are implemented.

4.1. Intervention scenarios

The five intervention scenarios analyzed herein are: (I) Riparian setbacks in the flood-prone area; (II) green urban development measures (GUD); (III) GUD measures combined with riparian setbacks in the flood prone area; (IV) GUD measures combined with an off-line detention basin; and (V) GUD measures combined with the detention basin and the riparian setbacks in the flood-prone area. These scenarios reduce exposure to flooding, flood hazard, or both (Table 3). Removing people from flood-prone areas within riparian setback buffers reduces

Table 3
Estimated initial costs and expected annual losses of scenarios.

		Exposure reduction →			
		No setbacks in flood-prone areas		People and structures removed from flood-prone areas in setbacks	
↓ Hazard reduction	No intervention	**Scenario 0**		**Scenario 1**	
		C_0	–	C_0	US$ 62.6 million
		EAL	US$ 47.30 million	EAL	US$ 37.24 million
	GUD interventions	**Scenario 2**		**Scenario 3**	
		C_0	US$ 84.2 million	C_0	US$ 138.5 million
		EAL	US$ 28.87 million	EAL	US$ 23.16 million
	GUD combined with flood-plain storage	**Scenario 4**		**Scenario 5**	
		C_0	US$ 124 million	C_0	US$ 178.5 million
		EAL	US$ 27.78 million	EAL	US$ 21.64 million

the number of people and structures exposed to flooding. Implementing GUD and additional storage interventions lowers the flood hydrograph and reduces flood hazard.

Table 3 shows initial costs (C_0) and *EAL* for each scenario, with *EAL* calculated as described in Section 3, by either implementing the mitigation strategies in the hydrological-hydraulic routine or changing the exposed assets.

4.1.1. Scenario 1: resettlement from flood-prone areas

This scenario consists of relocating structures from flood-prone areas along the Msimbazi river in the flood modeling domain. Relocation away from riparian areas historically has been a traditional flood damage mitigation strategy. Direct relocation costs can readily be quantified using World Bank compensation costs for the value of dwellings and other structures and land improvements (tree crops, agriculture) plus an 8% disturbance allowance to support households during the resettlement process [47]. We do not consider any psychological suffering or anxiety such relocation may impose on the affected individuals, or any reduction in flooding-related suffering avoided as a result of the relocation. There are 2422 structures at risk in the buffer zone that would be relocated, or approximately 20% of the entire portfolio of 12,744 structures at risk in the flood modeling domain. Direct relocation cost plus demolition cost (assumed to be 10% of the value of structures) is estimated at US$62.6 million. This scenario results in an *EAL* that is 21% lower than in Scenario 0.

4.1.2. Scenario 2: green urban development

The flood mitigation measures implemented in this scenario aim to reduce the heights of the hydrographs entering the flood modeling domain (green dots in Fig. 7b); their impact is modeled as described in Section 3.1.2.

The locations and extent of each physical intervention was estimated using landcover and the DEM. The costing of the selected interventions was based on a wide range of information sources collated from literature and various green urban development projects from other parts of the world. A detailed presentation of implementation characteristics, hydrologic impacts and costs for the GUD scenario can be found in Turpie et al. [47]. The total initial investment cost of the GUD interventions was estimated to be approximately $40 million with annual maintenance costs of about $1.6 million, with an additional 1% and 5% of the initial cost for inspection and maintenance, respectively. Mixed-use enhanced riparian and floodplain areas, which cover almost 500 ha and would detain 5 million m^3 of runoff, account for slightly more than 40% of the total cost of the GUD scenario. These interventions also require a resettlement of housing structures currently located in the intervention areas, with estimated resettlement costs, calculated analogously to Scenario 1, of US$ 44 million resulting in total initial costs of approximately US$ 84 million. Table 4 shows the breakdown of the extent and estimated costs of the individual GUD intervention components.

The reduction in discharge volume due to the improved soil infiltration and floodplain storage results in a reduction of the number of buildings at risk and, consequently, of *EAL* by approximately 39% compared to Scenario 0.

Table 5
Breakdown of the estimated costs of the off-line storage basin.

Cost component	Unit	Unit cost (US $ / unit)	Component subtotal (10^6 US$)
Purchase of land	50 ha	1000 $/ha	0.05
Excavation (90% of total volume)	2.7×10^6 m^3	8.6 $/$m^3$	23
Concrete works	20×10^3 m^3	255 $/$m^3$	5.1
Labor force (730 days)	100 people	8.48 $/day	0.62
Total direct input cost			**≈ 29**
Total cost including indirect and contingency costs of 36%			**≈ 40**

4.1.3. Scenario 3: green urban development and resettlement from flood-prone areas

This scenario combines Scenarios 1 and 2 and has an estimated initial cost of US$ 138.5 million. Total intervention cost is less than the sum of the costs of Scenarios 1 and 2 because in this scenario, the GUD interventions reduce the extent of the flood-prone area and therefore the number of structures at risk in the flood-prone areas compared to Scenario 1, resulting in fewer structures requiring relocation. Inspection and maintenance costs are the same as in Scenario 2. Scenario 3 reduces *EAL* by an estimated 51% compared to Scenario 0.

4.1.4. Scenario 4: green urban development and flood-storage basin

The lower part of the Msimbazi river catchment features an undeveloped area in the floodplain that we identified as a potential site for an off-line flood storage basin. We designed this basin based on Topa et al. [87]. With a 6-m depth, the 50-ha area allows the storage of 3 million cubic meters at an estimated initial cost (calculated using local construction costs; see Appendix B) of US$ 40 million (Table 5), including a contingency and indirect cost multiplier of 36% (Appendix B).

Scenario 4 has an initial estimated cost of US$ 124 million. Inspection and maintenance costs are higher than in Scenario 3, with an additional 1% and 5%, respectively, of the initial cost of the flood storage basin.

The implementation of the storage basin is modeled by reducing the discharge volume in the final part of the first inundation subdomain. Scenario 4 reduces *EAL* by 41% compared to Scenario 0.

4.1.5. Scenario 5: green urban development, resettlement from riverine buffer, and flood-storage basin

This Scenario is the combination of Scenarios 1 and 4, and its total initial cost is the sum of the cost of Scenario 3 and the cost of the flood storage basin, or US$ 178.5 million. Maintenance and inspection costs are the same as in Scenario 4. Scenario 5 reduces *EAL* by 54% compared to Scenario 0.

Table 4
Breakdown of the estimated extent and cost of the proposed GUD interventions.

Interventions	Extent (ha)	Initial cost (10^6 US$)	Maintenance (10^5 US$/yr)
Swales to improve drainage in flood prone areas	10	1.800	1.080
Catchment reforestation in Pugu Forest Reserve	776	0.845	0.170
Mixed use enhanced riparian and floodplain areas (~1 m deep)	488	28.00	10.360
Rehabilitated floodplain; wetland park (~2 m deep)	15	3.130	0.940
Enhanced floodplain-recessed gardens (~1 m deep)	51	5.360	1.070
Community-based river cleaning project		1.000	2.500
Total without resettlement costs	1340	40.135	16.12
Resettlement from the intervention areas		44	
Total with maximum resettlement costs		84.135	16.12

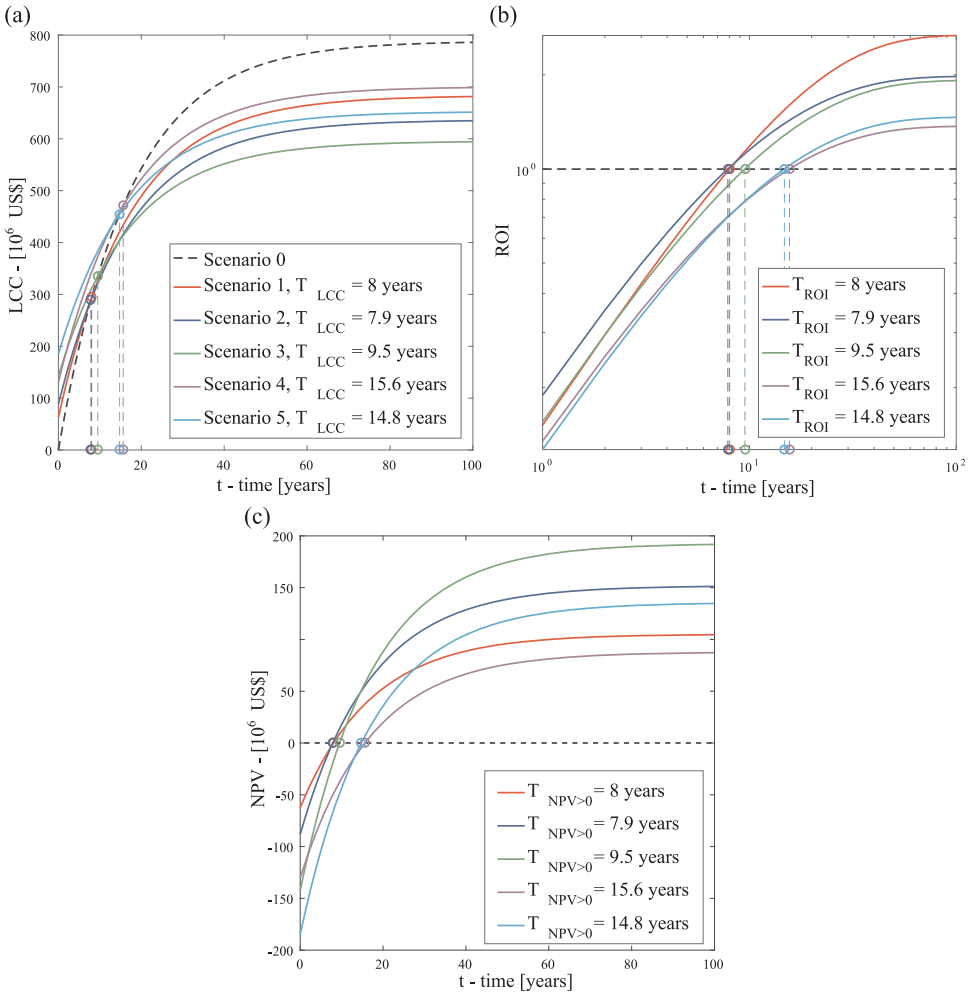

Fig. 10. (a) LCC, (b) ROI, and (c) NPV curves of the scenarios analyzed as a function of time.

4.2. Comparison of LCC and ROI of scenarios

All intervention scenarios significantly reduce *EAL* from flooding in the flood-prone areas of the lower Msimbazi catchment compared to the base case, with average annual costs declining by between $10 million and $26 million, or 21% and 54% of current *EAL* (Table 3). Fig. 10 shows LCC (Fig. 10a) and ROI (Fig. 10b) as a function of time for the five intervention scenarios analyzed. Note that the time scale of ROI is represented in log-scale to facilitate near-term performance comparisons.

While costs vary widely among the intervention scenarios, all have relatively short payback periods ranging from less than 8 to less than 16 years (Fig. 10). Scenarios 2 and 1 have the shortest payback period and the highest ROI, respectively, while Scenarios 3 and 4 have the lowest and highest LCC and thus generate the highest and lowest net present value, respectively.

These results underline the complementary nature of the LCC and ROI metrics. While ROI identifies the efficient alternative, that is, the one with the highest ratio of benefits to costs, it does not indicate the absolute size of the net benefits (NPV) of each alternative. For example, riparian setbacks with resettlement (Scenario 1) have the highest ROI of the alternatives analyzed for time horizons exceeding 8 years. However, the GUD measures bundle (Scenario 2) has a higher NPV than riparian setbacks because the difference between its LCC and that of the base case (Scenario 0) is larger than the difference between setback and base case LCCs. The choice between scenarios will depend on the size of the available initial intervention budget. Budget permitting, Scenario 3 is the preferred alternative on economic grounds as it generates the highest present value net benefits. In addition to the availability of financial resources, factors such as the desired length of the payback period, impacts on other ecosystem services in addition to flood mitigation and their respective values, and social equity concerns, should also be considered at the actual intervention design stage. Note that the NPVs of our scenarios are identical to the difference in the LCC costs of scenarios compared to those of the baseline scenario only because we do not include benefits other than avoided flood damages. Once any additional benefits are included in the analysis, NPV becomes a crucial additional metric to consider alongside LCC and ROI when selecting the preferred policy alternative or combination.

4.3. Conservative bias in our LCC and ROI estimates

It is worth noting that our LCC and ROI estimates likely are conservative for two reasons: first, they only account for reduced flood damages to buildings, ignoring other flood reduction benefits in the form of reductions in business and traffic interruption losses, public infrastructure damage, health costs and human suffering [88,89]. Second, they ignore the large projected future increases in urban flood damages due to socio-economic development [90].

Available models for assessing the indirect costs of riverine flooding at the city scale are fairly complex and data-demanding [89]. Consequently, indirect losses from river flooding are notoriously difficult to estimate [88], and very few damage assessments extend beyond direct structural flood impacts. Nevertheless, here we attempt to provide some

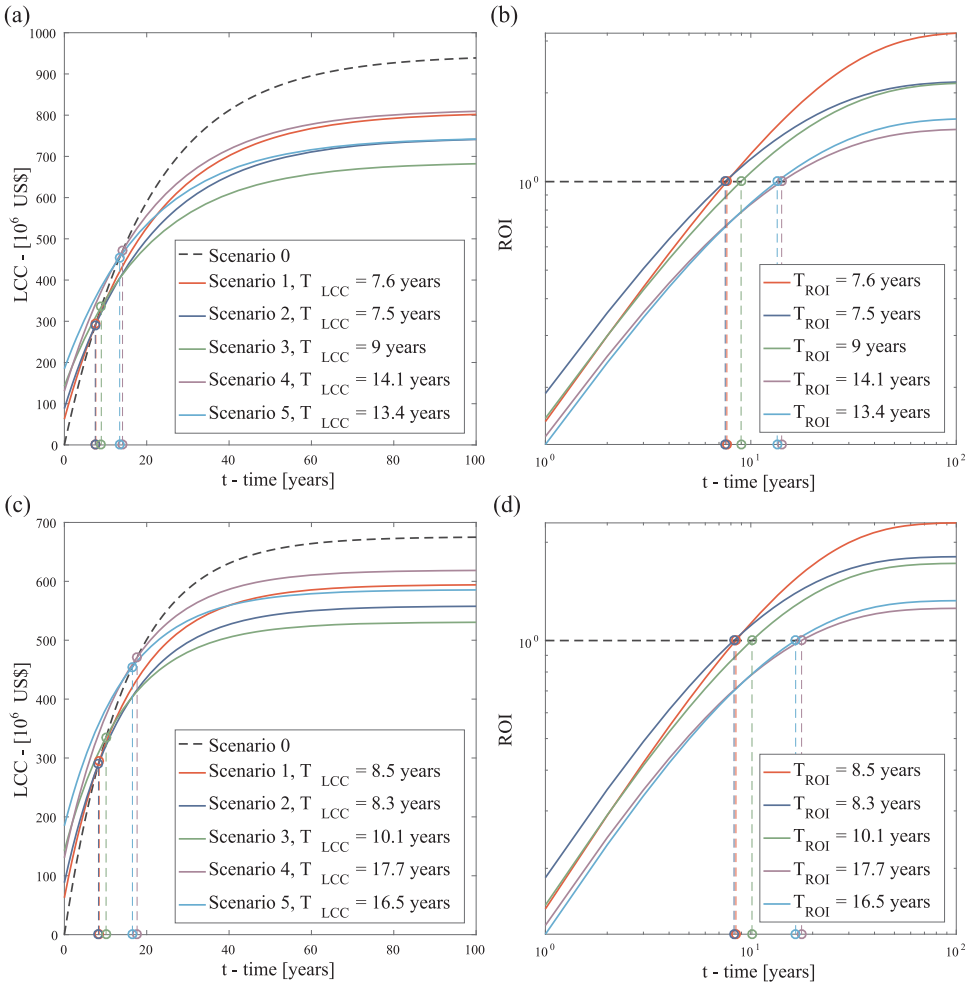

Fig. 11. (a,c) LCC and (b,d) ROI curves for the proposed scenarios for different discount rates: (a,b) 5% and (c,d) 7%.

perspective on the relative size of flood damages not captured in our analysis.

A survey of river flood-affected households and business units in Jakarta, Indonesia [91] found that structural damages accounted for only 14% of total damages while content damages (physical objects in and around buildings) accounted for 63% and indirect damages (clean-up cost, temporary housing, cost of illness, lost income) for 24%. Carrera et al. [92] used a computable general equilibrium (CGE) model to estimate the direct (structural damages) and indirect impacts (business interruption losses and associated ripple effects through the economy) of the 2000 Po river flood in Northern Italy. They estimated that indirect impacts were approximately 20% of direct impacts. Note however that their direct impacts include damages to all infrastructure, not just to residential and commercial buildings as in our and Wijavanti et al.'s [91] analyses, while their indirect impacts exclude losses from traffic interruptions, mortality and morbidity. Given the widespread annual flooding of Dar es Salaam's central business district and key transport lines and the fatalities and disease outbreaks related to flooding, impacts on both traffic and human life and health likely are important in the city. While ratios of direct to indirect flood damages depend on the local context, Wijayanti et al.'s [91] and Carrera et al.'s [92] results suggest that the direct damages to buildings – the only type of damage included in our analysis – may account for less than half of the total costs of flooding in Dar es Salaam. Thus, the actual ROI and NPV of our intervention scenarios may be twice as large as our estimates.

A review of published reports and newspaper articles indicates that during December 2011 and October 2017, an estimated 14 fatalities occurred on average per year in Dar es Salaam that were directly flood-related. Assuming that in Tanzania the shape of the value of remaining life years function is similar to the US [93] and that most flood-related fatalities occur in children and people of working age, the value of a statistical life (VSL) can serve as a rough approximation of the value of remaining life years. Using a VSL estimate for Tanzania of USD 158,000 [94], the total economic value of directly flood-related deaths in Dar es Salaam in recent years is an estimated USD 2.2 million per year on average.

Applying a cost-of-illness approach, it is also possible to construct an approximate estimate of the morbidity cost of flood-related cholera outbreaks in Dar es Salaam. Using high temporal resolution datasets on cholera cases and precipitation (a commonly used proxy for flooding [95]), Picarelli et al. [96] find a statistically highly significant ($p = 0.01$) link between extreme rainfall and cholera cases in Dar, with each additional week of top-quartile precipitation increasing the number of effective cholera cases by 20.3% relative to a week with very light rain, and by 22% in wards at greater risk of flooding. Importantly, Picarelli et al. [96] find no statistically significant link between a dry week and cholera in Dar. Trærup et al. [97] report an average public health care services cost per cholera case in Tanzania of USD 98 and an average stay of 5 days in isolation units. Using the unweighted mean of the monthly Tanzanian wage rates of the self-employed (USD 56/month), formal employees (USD 72/month) and the unemployed (USD 37/month) [97] and assuming 26 work days per month, and further assuming the 5000 cholera cases reported in Dar es Salaam during the 2015–2016 outbreak [96] are representative of the average annual number of cholera cases in the city, the total morbidity-related cost of illness from cholera in Dar is at least USD 0.55 million per year. This number is a low estimate because it does not include any private medical costs from cholera and only includes officially reported cholera cases.

The literature [51,52] suggests a correlation between human casualties and damages to the built environment. If the reduction in cholera cases and flood-related deaths in the intervention scenarios is roughly proportional to the reduction in estimated annual losses to buildings, the preferred intervention scenario (scenario 3) would be expected to reduce flooding-related mortality and morbidity costs by about 50%, or USD 1.4 million per year. This estimate does not include the cost associated with indirect deaths from flood-related morbidity effects or unreported deaths due to flooding, deaths due to cholera, or medical and productivity losses from flood-related injuries or illnesses other than cholera.

4.4. Sensitivity analysis

To assess the robustness of our results we conducted a sensitivity analysis of two key parameters, the discount rate and the inspection and maintenance costs of interventions. Using alternative discount rates of 5% and 7%, respectively (Fig. 11), does not affect the ranking of mitigation strategies; therefore, the general conclusions presented in Section 4.2 remain valid. Higher discount rates will lower LCC, net present value and ROI (due to the different time profiles of costs and benefits) and increase the payback period, while lower rates have the opposite effect.

Halving (Figs. 12a and 12b) or doubling (Figs. 12c and 12d) inspection and maintenance costs strongly affects the LCC and ROI of scenarios 2–5 and changes the LCC ranking except for Scenario 3, which remains the alternative with the highest net present value. A doubling of inspection and maintenance costs increases payback periods (substantially so for Scenarios 4 and 5) and LCC and reduces ROI, with Scenario 4 no longer superior to the base case (Scenario 0) but Scenario 2 remaining the second-best alternative in terms of LCC. Under halving of inspection and maintenance costs, Scenario 5 (all interventions combined) displaces Scenario 2 as the second-best LCC performer.

4.5. Omitted environmental and social impacts

This study focuses on evaluating the financial feasibility of the flood mitigation scenarios and their net benefits from avoided structural damages to buildings. It should be complemented by an environmental and social impact assessment (ESIA) to identify potential risks of undesirable distributional impacts especially on disadvantaged and vulnerable communities. Such assessments by now are widely applied by multilateral donors, international agencies and private lending institutions [45] and have the purpose of evaluating project impacts on biodiversity; risks to affected communities from changes in ecosystem services and resulting human welfare impacts; and risks arising from involuntary resettlement and economic displacement. While an ESIA is beyond the scope of our analysis, here we highlight the expected main environmental and social impacts of the analyzed flood mitigation scenarios.

All but one of those scenarios include large-scale “nature-based” interventions such as riparian and upland forest restoration and conservation, and “semi-natural” interventions such as reconnected, multi-use vegetated floodplains with riparian forest buffers and a river cleaning program. Compared to the business-as-usual scenario, these interventions are expected to improve upland forest habitat and reduce sediment, nutrient, bacterial and solid waste loadings of urban waterways, as well as providing significant amenity value. Thus, we expect strictly positive environmental impacts (on biodiversity and water

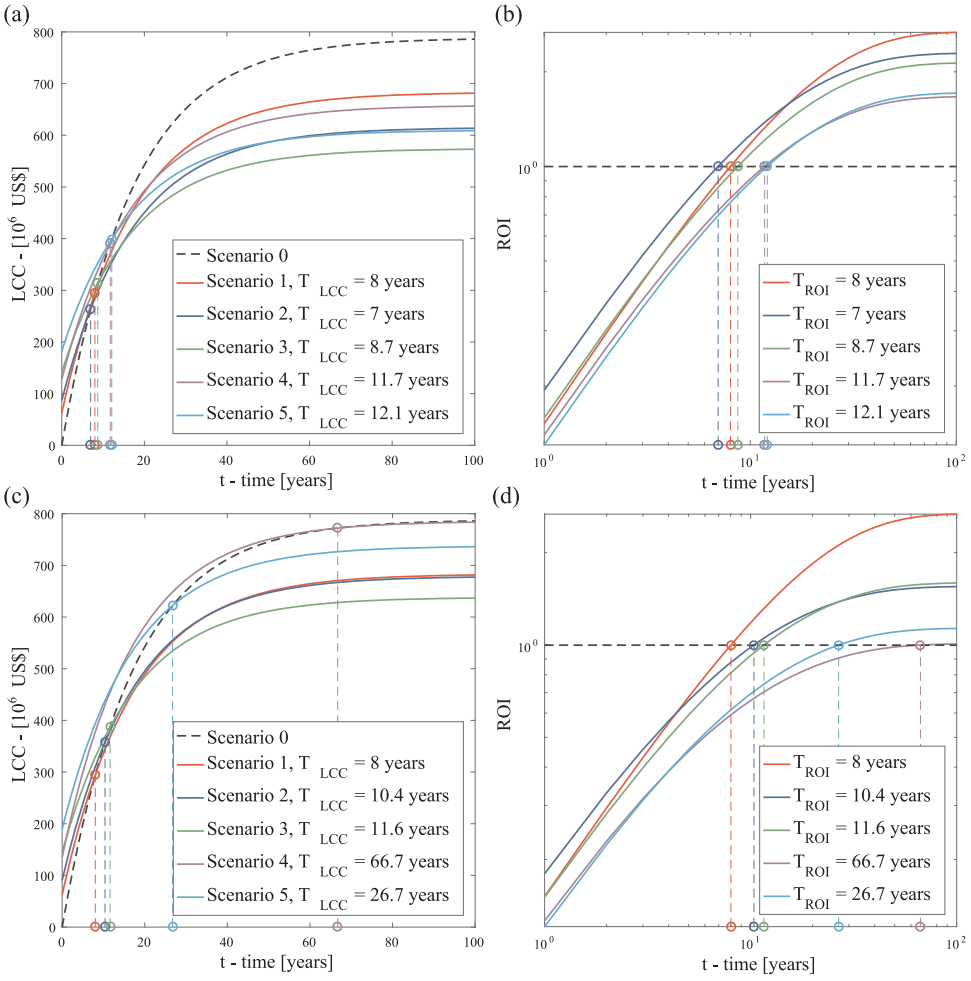

Fig. 12. Present value (a,c) LCC and (b,d) ROI curves for the analyzed scenarios for (a,b) half and (c,d) double inspection and maintenance costs.

quality) for the intervention scenarios that include nature-based components – that is, the ones preferred on LCC, ROI and NPV grounds.

Reductions in recurring damages to life and health (see Section 4.3) and to property from flooding produce welfare gains for local residents. The reduced sediment, nutrient, bacterial and solid waste loadings expected under all intervention scenarios may or may not be sufficient to reduce the incidence of waterborne diseases in people in direct contact with the river, but they certainly will not increase it. Riparian forest buffers and multi-use floodplains will enhance the scarce recreational opportunities available for nearby residents as well as increase food production, again positively impacting livelihoods. However, some of these welfare and livelihood gains may be partially offset by any negative livelihood impacts sustained by households who are resettled from flood-prone areas. Such impacts may occur for households who experience net income losses from resettlement that are not offset by their resettlement compensation. Clearly, this last issue points to the need to complement our analysis by a social impact assessment.

5. Summary and conclusion

We present a new approach for quantifying and communicating urban-scale flood risk and mitigation strategies in developing countries that uses a performance-based engineering approach and probabilistic Life Cycle Cost and Return on Investment as decision variables. We apply this approach to a case study that demonstrates the usefulness and complementarity of LCC and ROI as decision variables for selecting flood risk mitigation strategies, and their superiority over decision making that considers only the initial cost of mitigation interventions.

We analyze a range of green urban development interventions that would mitigate flood damages in Dar es Salaam by reducing either exposure to flooding, flood hazard, or both. All scenarios outperform the status quo base case (reducing *EAL* by 21–54%) and generate net welfare gains. Absolute benefits (avoided flood damages) increase with scenarios that include successively more comprehensive bundles of the analyzed mitigation measures, but so do intervention costs (with initial costs ranging from US$ 62.6–178.5 million). Among individual measures, catchment rehabilitation was found to provide higher net benefits, outperforming resettlement of people from flood-prone areas or construction of a large flood storage basin, and had the shortest payback period (7.9 years). The flood storage basin provided the lowest flood damage reduction benefit, largely because opportunities for siting such a basin were too far downstream in the catchment to be particularly effective. Increasing the discount rate decreases the Life Cycle Cost and increases the payback period while leaving the ranking of alternatives unaffected. On the other hand, increasing the size of inspection and maintenance costs increases both LCC and payback period and affects the ranking of alternatives.

Our results suggest that a combination of measures designed to attenuate flows and improve drainage should be implemented that includes improved solid waste management and community-based river cleaning programs, reforestation in the upper catchment, the rehabilitation of river buffers in the middle catchment and the reconnection of floodplains in the lower reaches that are redesigned for both flood storage and flooding-compatible additional uses including agriculture and recreation. This could be part of an even broader catchment-to-coast rehabilitation program for the Msimbazi River system that also aims to address water quality problems and the need for green open space within the rapidly-growing city.

Due to limited data availability, this study utilized simple models and assumptions for the hydrologic analysis. Investment in the development of better hydrological data, through establishment of high temporal resolution stream flow and additional rainfall gauges, and detailed spatial datasets on soils, land cover, the built environment and the city's subsurface drainage systems are needed to reduce uncertainties in our results. In addition, future work should focus on mapping actual flood footprints and associated housing and infrastructure damages to allow model calibration. While our results are preliminary and warrant further study, they nevertheless strongly suggest that catchment rehabilitation interventions are likely to yield substantial economic net benefits in Dar es Salaam from reduced building damages from flooding alone. This means there exists economic justification for moving towards a greener flood management approach for the city. While the latter likely would yield important social and environmental co-benefits and associated welfare gains [44], its implementation must be preceded by a social impact assessment to identify and mitigate any negative impacts on disadvantaged and vulnerable urban sectors.

Acknowledgements

This work was supported by funding from the World Bank Project “Promoting Green Urban Development in Africa”, The Nature Conservancy”, the Environment for Development Initiative and the Sage Foundation.

Appendix A

Two main sources have been used: the National Construction Council of Tanzania (www.ncc.org.zm) and the 26th edition of annual African Property and Construction Handbook (http://www.coolrooftoolkit.org/wp-content/uploads/2014/07/AEcomConstructionHandbookFinal_v2.pdf) released by AECOM (Table A1).

Table A1
Unit costs for building type.

Building type	Unit cost US$/m^2
Swahili house	100
Bungalow, corrugated iron sheet roofing	120
Bungalow, tiled roof	150
Bungalow, slab roof	180
Maisonette double storey, slab roof	170
Flats	150
Residential average multi-unit high-rise	667
Residential Luxury unit high rise	894
Residential Individual prestige house	964
Commercial Standard office high rise	823
Commercial Prestige office high rise	1041
Commercial Major shopping center	765
Industrial light duty factory	616
Industrial heavy duty factory	1100
Car park	490

Appendix B

This section focuses on the costs of construction, such as the land purchase, earthwork, etc. The values reported below present the information collected from the Tanzania National Construction Council and from the study of different ongoing projects in Dar es Salaam.

The transport to the waste treatment plant of the removed soil/derbies is assumed having a percentage of 10% of the total earthwork cost.

To the input costs listed in Tables B1–B3 we added overhead costs expressed as a percentage of total input cost. Table B4 below lists these overhead costs by type as a percentage of the total civil works input cost.

Table B1
Unit costs for basic construction work item.

Work item	Description	Unit cost
Purchase of land		1000 $/ha
Earthwork	Excavation	8.6 $/m^3
	Embankment	12.8 $/m^3
Concrete work		255 $/m^3

Table B2
Unit costs for basic construction materials.

Material item	Unit	Unit cost $
Gasoline	Liter	0.69
Diesel	Liter	0.67
Portland cement	1000 kg	98.62
Reinforcement bar	1000 kg	495.62
Fine aggregate	m^3	10.39
Coarse Aggregate	m^3	21.82
Plywood	m^2	23.85
Timber	m^3	286.15
Wooden pile	m	7.95
Wood	m^3	238.46

Table B3
Unit costs for daily labor wage considering social insurance, overtime, layoff allowance and retirement allowance.

Labor	Unit cost $
Foreman	8.48
Skilled labor	4.43
Common labor	3.64
Unskilled labor	2.91
Operator for heavy equipment	8.02
Driver for light vehicle	7.64
Carpenter	6.75
Welder	9.35
Mechanic	9.70
Electrician	10.39

Table B4
Additional costs: percentage of the total civil work cost.

Labor	Percentage respect to the total cost of the civil works
Preparation works	7%
Contractor's indirect costs	10%
Engineering service	7%
Contingency	10%
Government administration cost	2%

References

[1] National Research Council, Facing Hazards and Disasters: Understanding Human Dimensions, The National Acadamies Press, Washington DC, USA, 2006, p. 408.
[2] F. Al-Nammari, M. Alzaghal, Towards local disaster risk reduction in developing countries: challenges from Jordan, Int. J. Disaster Risk Reduct. 12 (2015) 34–41.
[3] R. De Risi, F. Jalayer, F. De Paola, I. Iervolino, M. Giugni, M.E. Topa, E. Mbuya, A. Kyessi, G. Manfredi, P. Gasparini, Flood risk assessment for informal settlements, Nat. Hazards 69 (1) (2013) 1003–1032.
[4] L.B. Herslund, F. Jalayer, N. Jean-Baptiste, G. Jørgensen, S. Kabisch, W. Kombe, S. Lindley, P.K. Nyed, S. Pauleit, A. Printz, T. Vedeld, A multi-dimensional assessment of urban vulnerability to climate change in sub-Saharan Africa, Nat. Hazards 82 (2) (2016) 149–172.
[5] F. Jalayer, R. De Risi, A. Kyessi, E. Mbuya, N. Yonas, Vulnerability of built environment to flooding in african cities. Chapter 3 of: urban vulnerability and climate change in Africa, in: S. Pauleit, et al. (Ed.), Future City, 4 Springer International Publishing, Switzerland, 2015, pp. 77–106.

[6] D. Feldman, S. Contreras, B. Karlin, V. Basolo, R. Matthew, B. Sanders, D. Houston, W. Cheung, K. Goodrich, A. Reyes, Communicating flood risk: looking back and forward at traditional and social media outlets, Int. J. Disaster Risk Reduct. 15 (2016) 43–51.

[7] S. Deen, Pakistan 2010 floods. policy gaps in disaster preparedness and response, Int. J. Disaster Risk Reduct. 12 (2015) 341–349.

[8] F. Jalayer, R. De Risi, F. De Paola, M. Giugni, G. Manfredi, P. Gasparini, M.E. Topa, N. Yonas, K. Yeshitela, A. Nebebe, G. Cavan, Probabilistic GIS-based method for delineation of urban flooding risk hotspots, Nat. Hazards 73 (2) (2014) 975–1001.

[9] S. Kumar, R. Diaz, J.G. Behr, A.L. Toba, Modeling the effects of labor on housing reconstruction: a system perspective, Int. J. Disaster Risk Reduct. 12 (2015) 154–162.

[10] C.P. Castro, I. Ibarra, M. Lukas, J. Ortiz, J.P. Sarmiento, Disaster risk construction in the progressive consolidation of informal settlements: iquique and Puerto Montt (Chile) case studies, Int. J. Disaster Risk Reduct. 13 (2015) 109–127.

[11] R. De Risi, F. Jalayer, I. Iervolino, G. Manfredi, S. Carozza, VISK: a GIS-compatible platform for micro-scale assessment of flooding risk in urban areas, In: COMPDYN, 4th ECCOMAS Thematic Conference on Computational Methods in Structural Dynamics and Earthquake Engineering. Kos Island, Greece.

[12] T. Sakijege, J. Sartohadi, M.A. Marfai, G.R. Kassenga, S.E. Kasala, Assessment of adaptation strategies to flooding: a comparative study between informal settlements of Keko Machungwa in Dar es Salaam, Tanzania and Sangkrah in Surakarta, Indonesia, Jàmbá: J. Disaster Risk Stud. 6 (1) (2014) 1–10.

[13] M. Nkwenkeu, C. Pettang, P. Louzolo-Kimbembè, Cartography of the segregation as a tool of decision-making aid for the fight against poverty: case of the town of Yaounde (Cameroon), Build. Environ. 40 (10) (2005) 1375–1383.

[14] C. Pettang, T.T. Tatietse, A new proposition for the curbing of spontaneous housing in urban area in Cameroon, Build. Environ. 33 (4) (1998) 245–251.

[15] S. Khan, I. Kelman, Progressive climate change and disasters: connections and metrics, Nat. Hazards 61 (3) (2012) 1477–1481.

[16] F. Jalayer, R. De Risi, G. Manfredi, F. De Paola, M.E. Topa, M. Giugni, E. Bucchignani, E. Mbuya, A. Kyessi, P. Gasparini, From climate predictions to flood risk assessment for a portfolio of structures, In: Proceedings of the 11th International Conference on Structural Safety & Reliability (ICOSSAR 2013), Columbia University, New York, NY, June 16-20, 2013.

[17] D. Ocio, C. Stocker, Á. Eraso, A. Martínez, J.M.S. de Galdeano, Towards a reliable and cost-efficient flood risk management: the case of the Basque Country (Spain), Nat. Hazards 81 (1) (2016) 617–639.

[18] H. Apel, G. Aronica, H. Kreibich, A. Thieken, Flood risk analyses—how detailed do we need to be? Nat. Hazards 49 (1) (2009) 79–98.

[19] I.M. Voskamp, F.H.M. Van de Ven, Planning support system for climate adaptation: composing effective sets of blue-green measures to reduce urban vulnerability to extreme weather events, Build. Environ. 83 (2015) 159–167.

[20] R.A.W. Albers, P.R. Bosch, B. Blocken, A.A.J.F. Van Den Dobbelsteen, L.W.A. Van Hove, T.J.M. Spit, V. Rovers, Overview of challenges and achievements in the climate adaptation of cities and in the climate proof cities program, Build. Environ. 83 (2015) 1–10.

[21] J.B. Marco, G. Rossi, N. Harmancioğlu, V. Yevjevich (Eds.), Flood Risk Mapping, Chapter 20 of: Coping with Floods, 257 Springer, Netherlands, 1994, pp. 353–373.

[22] B. Merz, A.H. Thieken, M. Gocht, S. Begum, M.F. Stive, J. Hall (Eds.), Flood Risk Mapping at the Local Scale: Concepts and Challenges. Chapter 13 of: Flood Risk Management in Europe, 25 Springer Netherlands, 2007, pp. 231–251.

[23] M.A.R. Shah, A. Rahman, S.H. Chowdhury, Challenges for achieving sustainable flood risk management, J. Flood Risk Manag. (2015), http://dx.doi.org/10.1111/jfr3.12211.

[24] W. Fabrycky, Concurrent Life-Cycle Engineering for the Optimization of Products, Systems, and Structures. In Modern Production Concepts, Springer Berlin Heidelberg, 1991, pp. 526–543.

[25] K.F. Liu, C.Y. Ko, C. Fan, C.W. Chen, Combining risk assessment, life cycle assessment, and multi-criteria decision analysis to estimate environmental aspects in environmental management system, Int. J. Life Cycle Assess. 17 (7) (2012) 845–862.

[26] Y. Dong, D.M. Frangopol, Probabilistic life-cycle cost-benefit analysis of portfolios of buildings under flood hazard, Eng. Struct. 142 (2017) 290–299.

[27] K. Goda, C.S. Lee, H.P. Hong, Lifecycle cost–benefit analysis of isolated buildings, Struct. Saf. 32 (1) (2010) 52–63.

[28] C. Menna, D. Asprone, F. Jalayer, A. Prota, G. Manfredi, Assessment of ecological sustainability of a building subjected to potential seismic events during its lifetime, Int. J. Life Cycle Assess. 18 (2) (2013) 504–515.

[29] S.E. Chang, M. Shinozuka, Life-cycle cost analysis with natural hazard risk, J. Infrastruct. Syst. 2 (3) (1996) 118–126.

[30] F. Jalayer, D. Asprone, A. Prota, G. Manfredi, Multi-hazard upgrade decision making for critical infrastructure based on life-cycle cost criteria, Earthq. Eng. Struct. Dyn. 40 (10) (2011) 1163–1179.

[31] D.M. Frangopol, K.Y. Lin, A.C. Estes, Life-cycle cost design of deteriorating structure, ASCE J. Struct. Eng. 123 (10) (1997) 1390–1401.

[32] D.M. Frangopol, M.J. Kallen, J.M. Noortwijk, Probabilistic models for life-cycle performance of deteriorating structures: review and future directions, Progs. Struct. Eng. Mater. 6 (2004) 197–212.

[33] M.H. Faber, R. Rackwitz, Sustainable decision making in civil engineering, Struct. Eng. Int. 3 (2004) 237–242.

[34] B.R. Ellingwood, Y.K. Wen, Risk-benefit-based design decisions for low-probability/high consequence earthquake events in Mid-America, Prog. Struct. Eng. Mater. 7 (2005) 56–70.

[35] H.R. Sahely, C.A. Kennedy, B.J. Adams, Developing sustainability criteria for urban infrastructure systems, Can. J. Civil. Eng. 32 (1) (2005) 72–85.

[36] D.R. Godschalk, Urban hazard mitigation: creating resilient cities, Nat. Hazards Rev. 4 (3) (2003) 136–143.

[37] F.D. Mwale, A.J. Adeloye, L. Beevers, Quantifying vulnerability of rural communities to flooding in SSA: a contemporary disaster management perspective applied to the lower Shire Valley, Malawi, Int. J. Disaster risk Reduct. 12 (2015) 172–187.

[38] S. Rufat, E. Tate, C.G. Burton, A.S. Maroof, Social vulnerability to floods: review of case studies and implications for measurement, Int. J. Disaster Risk Reduct. 14 (2015) 470–486.

[39] F. Reilly, K. Brown, Investment Analysis and Portfolio Management, 10th ed., Cengage Learning, OH, 2011, p. 1080 (Mason).

[40] J. Boyd, R. Epanchin-Niell, J. Siikamäki. Conservation Return on Investment Analysis: A Review of Results, Methods, and New Directions. 2012. Resources for the Future Discussion paper 12-01.

[41] A.L. Vogl, B.P. Bryant, J.E. Hunink, S. Wolny, C. Apse, P. Droogers, Valuing investments in sustainable land management in the Upper Tana River basin, Kenya, J. Environ. Manag. 195 (2017) 78–91.

[42] T. Kroeger, G. Guannel, Fishery enhancement and coastal protection services provided by two restored Gulf of Mexico Oyster Reefs, in: K. Ninan (Ed.), Valuing Ecosystem Services-Methodological Issues and Case Studies. Edward Elgar, Cheltenham, 2014, pp. 334–358 (464 pp).

[43] T. Kroeger, F.J. Escobedo, J.L. Hernandez, S. Varela, S. Delphin, J.R.B. Fisher, J. Waldron, Reforestation as a novel abatement and compliance measure for ground-level ozone, Proc. Natl. Acad. Sci. 111 (40) (2014) E4204–E4213.

[44] R. White, J. Turpie, G. Letley, Greening Africa's Cities: Enhancing the Relationship Between Urbanization, Environmental Assets and Ecosystem Services, The World Bank©, Washington D.C., 2017, p. 50 〈https://openknowledge.worldbank.org/handle/10986/26730〉.

[45] B. Dendena, S. Corsi, The environmental and social Impact assessment: a further step towards an integrated assessment process, J. Clean. Prod. 108 (2015) 965–977.

[46] D. Guha-Sapir, R. Below, P.H. Hoyois, EM-DAT: International Disaster Database, 2015. Available at: 〈www.emdat.be〉. (Accessed 1 March 2016).

[47] J. Turpie, T. Kroeger, R. De Risi, F. De Paola, G. Letley, K. Forsythe, L. Day, Return on Investment in Green Urban Development: Amelioration of Flood Risk in the Msimbazi River Catchment, Dar es Salaam, Tanzania. Promoting Green Urban Development in Africa, World Bank, Washington DC, 2017〈https://openknowledge.worldbank.org/handle/10986/26702〉 (Accessed 1 June 2017).

[48] T. Leader, H.R. Wallingford, Language of Risk. Deliverable D32.2. FLOODsite project. 〈http://floodsite.net/html/partner_area/project_docs/T32_04_01_FLOODsite_Language_of_Risk_D32_2_v5_2_P1.pdf〉, (Accessed 1 March 2017).

[49] J.S. O'Brien, P.Y. Julien, W.T. Fullerton, Two-dimensional water flood and mudflow simulation, J. Hydraul. Eng. 119 (2) (1993) 244–261.

[50] E. Hagen, X.X. Lu, Let us create flood hazard maps for developing countries, Nat. Hazards 58 (3) (2011) 841–843.

[51] S.N. Jonkman, P.H.A.J.M. Van Gelder, J.K. Vrijling, An overview of quantitative risk measures for loss of life and economic damage, J. Hazard. Mater. 99 (1) (2003) 1–30.

[52] S.N. Jonkman, I. Kelman, An analysis of the causes and circumstances of flood disaster deaths, Disasters 29 (1) (2005) 75–97.

[53] K. Porter, R. Kennedy, R. Bachman, Creating fragility functions for performance-based earthquake engineering, Earthq. Spectra 23 (2) (2007) 471–489.

[54] S. Hallegatte, V. Przyluski, The Economics of Natural Disasters: Concepts and Methods. World Bank Policy Research Working Paper 5507. Washington DC: The World Bank. 〈https://openknowledge.worldbank.org/bitstream/handle/10986/3991/WPS5507.pdf〉, 2010.

[55] A. Pistrika, G. Tsakiris, I. Nalbantis, Flood depth-damage functions for built environment, Environ. Process. 1 (4) (2014) 553–572.

[56] C. Scawthorn, N. Blais, H. Seligson, E. Tate, E. Mifflin, W. Thomas, C. Jones, HAZUS-MH flood loss estimation methodology. I: Overview and flood hazard characterization, Nat. Hazards Rev. 7 (2) (2006) 60–71.

[57] C. Scawthorn, P. Flores, N. Blais, H. Seligson, E. Tate, S. Chang, M. Lawrence, HAZUS-MH flood loss estimation methodology. II. Damage and loss assessment, Nat. Hazards Rev. 7 (2) (2006) 72–81.

[58] K. Goda, H.P. Hong, Estimation of seismic loss for spatially distributed buildings, Earthq. Spectra 24 (4) (2008) 889–910.

[59] R. De Risi, K. Goda, N. Mori, T. Yasuda, Bayesian tsunami fragility modeling considering input data uncertainty, Stoch. Environ. Res. Risk Assess. 31 (5) (2016) 1253–1269.

[60] E.K. Lauritzen, Emergency construction waste management, Saf. Sci. 30 (1) (1998) 45–53.

[61] A. Bozza, D. Asprone, G. Manfredi, Developing an integrated framework to quantify resilience of urban systems against disasters, Nat. Hazards 78 (3) (2015) 1729–1748.

[62] ISO 15686-5, Buildings – Service life planning – Part 5: Life cycle costing. International Organization for Standardization, 2006.

[63] D. Arditi, H.M. Messiha, Life cycle cost analysis (LCCA) in municipal organizations, J. Infrastruct. Syst. 5 (1) (1999) 1–10.

[64] O. Salem, S. AbouRizk, S. Ariaratnam, Risk-based life-cycle costing of infrastructure rehabilitation and construction alternatives, J. Infrastruct. Syst. 9 (1) (2003) 6–15.

[65] J. Kong, D. Frangopol, Evaluation of expected life-cycle maintenance cost of deteriorating structures, J. Struct. Eng. 129 (5) (2003) 682–691.

[66] E.P. Fenichel, M.J. Kotchen, E. Addicott. Even the representative agent must die: Using demographics to inform long-term social discount rates, 2017. NBER Working Paper No. 23591. 〈http://dx.doi.org/10.3386/w23591〉. Available at: 〈http://www.nber.org/papers/w23591.pdf〉. (Accessed 1 October 2017).

[67] B.R. Ellingwood, Y.K. Wen, Risk-benefit-based design decisions for low-probability/high consequence earthquake events in Mid-America, Prog. Struct. Eng. Mater. 7 (2)

(2005) 56–70.
[68] F. De Paola, M. Giugni, M.E. Topa, E. Bucchignani, Intensity-Duration-Frequency (IDF) rainfall curves, for data series and climate projection in African cities, SpringerPlus 3 (1) (2014) 133.
[69] S. Pauleit, F. Duhme, Assessing the environmental performance of land cover types for urban planning, Landsc. Urban Plan. 52 (1) (2000) 1–20.
[70] E. Kuichling, The Relation Between the Rainfall and the Discharge of Sewers in Populous Districts 20 American Society of Civil Engineers, Transactions, 1889, pp. 1–56.
[71] V. Mockus, National Engineering Handbook, Section 4, Hydrology, US Soil Conservation Service, Washington, D.C., 1972.
[72] A.A. El-Nasr, J.G. Arnold, J. Feyen, J. Berlamont, Modelling the hydrology of a catchment using a distributed and a semi-distributed model, Hydrol. Process. 19 (3) (2005) 573–587.
[73] M.B. Smith, D.J. Seo, V.I. Koren, S.M. Reed, Z. Zhang, Q. Duan, S. Cong, The distributed model intercomparison project (DMIP): motivation and experiment design, J. Hydrol. 298 (1–4) (2004) 4–26.
[74] J.C. Refsgaard, J. Knudsen, Operational validation and intercomparison of different types of hydrological models, Water Resour. Res. 32 (7) (1996) 2189–2202.
[75] M. Mulligan, WaterWorld: a self-parameterising, physically based model for application in data-poor but problem-rich environments globally, Hydrol. Res. 44 (5) (2013) 748–769.
[76] L. Bharati, K.H. Lee, T.M. Isenhart, R.C. Schultz, Soil-water infiltration under crops, pasture, and established riparian buffer in Midwestern USA, Agrofor. Syst. 56 (3) (2002) 249–257.
[77] X.Y. Li, S. Contreras, A. Solé-Benet, Y. Cantón, F. Domingo, R. Lázaro, H. Lin, B. Van Wesemael, J. Puigdefábregas, Controls of infiltration–runoff processes in Mediterranean karst rangelands in SE Spain, Catena 86 (2) (2011) 98–109.
[78] R. Ruggenthaler, G. Meißl, C. Geitner, G. Leitinger, N. Endstrasser, F. Schöberl, Investigating the impact of initial soil moisture conditions on total infiltration by using an adapted double-ring infiltrometer, Hydrol. Sci. J. 61 (7) (2016) 1263–1279.
[79] K.K. Farrick, B.A. Branfireun, Soil water storage, rainfall and runoff relationships in a tropical dry forest catchment, Water Resour. Res. 50 (12) (2014) 9236–9250.
[80] G.J. Arcement, V.R. Schneider. Guide for selecting Manning's roughness coefficients for natural channels and flood plains, 1989. United States Geological Survey Water-Supply Paper 2339. Available at: 〈http://dpw.lacounty.gov/lacfcd/wdr/files/WG/041615/Guide%20for%20Selecting%20n-Value.pdf〉. (Accessed 1 June 2017).
[81] F. Jalayer, S. Carozza, R. De Risi, G. Manfredi, E. Mbuya, Performance-based flood safety-checking for non-engineered masonry structures, Eng. Struct. 106 (2016) 109–123.
[82] R. De Risi, A probabilistic bi-scale frame work for urban flood risk assessment (Ph.D. dissertation), Department of structures for Engineering and Architecture, University of Naples Federico II, Naples, 2013.
[83] S. Reese, B.A. Bradley, J. Bind, G. Smart, W. Power, J. Sturman, Empirical building fragilities from observed damage in the 2009 South Pacific tsunami, Earth-Sci. Rev. 107 (1) (2011) 156–173.
[84] I. Charvet, A. Suppasri, H. Kimura, D. Sugawara, F. Imamura, Fragility estimations for Kesennuma City following the 2011 Great East Japan tsunami based on maximum flow depths, velocities and debris impact, with evaluation of the ordinal model's predictive accuracy, Nat. Hazards 79 (3) (2015) 2073–2099.
[85] A. Suppasri, E. Mas, I. Charvet, R. Gunasekera, K. Imai, Y. Fukutani, F. Imamura, Building damage characteristics based on surveyed data and fragility curves of the 2011 Great East Japan tsunami, Nat. Hazards 66 (2) (2013) 319–341.
[86] D.J. Thampapillai, W.F. Musgrave, Flood damage mitigation: a review of structural and nonstructural measures and alternative decision frameworks, Water Resour. Res. 21 (4) (1985) 411–424.
[87] M.E. Topa, M. Giugni, F. De Paola, Off-stream floodplain storage: Numerical modeling and experimental analysis, J. Irrig. Drain. Eng. 141 (1) (2014) 04014040.
[88] B. Merz, H. Kreibich, R. Schwarze, A. Thieken, Assessment of economic flood damage, Nat. Hazards Earth Syst. Sci. 10 (8) (2010) 1697.
[89] M.J. Hammond, A.S. Chen, S. Djordjević, D. Butler, O. Mark, Urban flood impact assessment: a state-of-the-art review, Urban Water J. 12 (1) (2015) 14–29.
[90] H.C. Winsemius, J.C.J.H. Aerts, L.P.H. van Beek, M.F.P. Bierkens, A. Bouwman, B. Jongman, J.C.J. Kwadijk, W. Ligtvoet, P.L. Lucas, D.P. van Vuuren, P.J. Ward, Global drivers of future river flood risk, Nat. Clim. Change 6 (2016) 381–385.
[91] P. Wijayanti, X. Zhu, P. Hellegers, Y. Budiyono, E.C. van Ierland, Estimation of river flood damages in Jakarta, Indonesia, Nat. Hazards 86 (3) (2017) 1059–1079.
[92] L. Carrera, G. Standardi, F. Bosello, J. Mysiak, Assessing direct and indirect economic impacts of a flood event through the integration of spatial and computable general equilibrium modelling, Environ. Model. Softw. 63 (2015) 109–122.
[93] K. Murphy, R. Topel, The value of health and longevity, J. Polit. Econ. 114 (5) (2006) 871–904.
[94] W.K. Viscusi, C.J. Masterman, Income elasticities and global values of a statistical life, J. Benefit Cost Anal. 8 (2) (2017) 226–250.
[95] J.J. Chen, V. Mueller, Y. Jia, S.K.H. Tseng, Validating migration responses to flooding using satellite and vital registration data, Am. Econ. Rev. 107 (5) (2017) 441–445.
[96] N. Picarelli, P. Jaupart, Y. Chen, Cholera in Times of Floods: Weather Shocks and Health in Dar es Salaam, International Growth Centre, London School of Economics, 2017 (Working Paper C-40404-TZA-1.
[97] S.L.M. Trærup, R.A. Ortiz, A. Markandya, The costs of climate change: a study of cholera in Tanzania, Int. J. Environ. Resour. Public Health 8 (2011) 4386–4405.